NACA TN 4128 10463

TECH LIBRARY KAFB, NM
0066880

NATIONAL ADVISORY COMMITTEE FOR AERONAUTICS

TECHNICAL NOTE 4128

A THERMOCOUPLE SUBCARRIER OSCILLATOR FOR TELEMETERING TEMPERATURES FROM PILOTLESS AIRCRAFT

By Clifford L. Fricke

Langley Aeronautical Laboratory
Langley Field, Va.

Washington
December 1957

AFMDC
TECHNICAL LIBRARY
AFL 2811

TECH LIBRARY KAFB, NM
0066880

L

NATIONAL ADVISORY COMMITTEE FOR AERONAUTIC

TECHNICAL NOTE 4128

A THERMOCOUPLE SUBCARRIER OSCILLATOR FOR TELEMETERING TEMPERATURES FROM PILOTLESS AIRCRAFT

By Clifford L. Fricke

SUMMARY

A subcarrier oscillator was designed which, in conjunction with the NACA telemetering system, gives a satisfactory method for telemetering temperatures by means of thermocouples from pilotless aircraft. The design uses a diode-bridge modulator in conjunction with a phase-shift oscillator; the thermocouple voltage is changed to alternating current and is used to shift the phase and hence to change the frequency of oscillation. This method results in an oscillator having a small size, low microphonics, high input resistance, and satisfactory stability if a switch is used to commutate calibration voltages along with the pickups.

INTRODUCTION

One of the major problems in the design of supersonic aircraft is aerodynamic or friction heating (ref. 1). A realistic method of investigating aerodynamic phenomena that is employed by the NACA uses rocket-propelled pilotless-aircraft test vehicles. These research missiles are propelled to the supersonic speeds necessary to study friction heating as well as other aerodynamic quantities (ref. 2). On all these models, measurements must be remote since models are not recoverable. Acceleration, velocity, and position in space can be determined by radar, but other measurements must be telemetered - that is, relayed to a ground station by radio transmission. Heat transfer from the boundary layer to the skin is determined from the rate of change of skin temperature. Boundary-layer temperatures are usually calculated, but skin temperatures must be measured.

In the past, a resistance-type temperature telemeter has been used with success below 600° F (ref. 3). At high temperatures, cements used to bond the wire to the skin either fail to hold the wire to the skin or do not insulate properly. In addition, difficulty in installation and calibration make such a system undesirable. On the other hand, thermocouple pickups are easily attached to skin surfaces and calibrations need be made only on a sample of wire. For missiles where several

pickups are required, these advantages are very important. However, a thermocouple electromotive force, being small, is difficult to telemeter, and in the past a thermocouple telemeter suitable for use in small missiles has not been available.

Thus, in order to establish very essential design data and aerodynamic heating theories, the telemetering of temperatures from high-speed pilotless aircraft is required. A small thermocouple telemeter is needed which will give accurate data under high ambient temperatures and accelerations. This report discusses the problem involved in the design of such a telemeter and describes a thermocouple subcarrier oscillator used by the Langley Aeronautical Laboratory. The material presented herein was submitted to the University of Virginia in partial fulfillment of the requirements for the degree of Master of Electrical Engineering.

SYMBOLS

A^+	d-c heater supply, v
B^+	d-c plate supply, v
C	tank capacitance, f
C_k	cathode capacitance in first stage, f
C_u	unbalancing capacitance, f
C_u'	unbalancing capacitance across unbalancing inductance, f
E_1	peak-to-peak a-c voltage input to driver stage, v
E_g	peak-to-peak a-c grid to cathode voltage of driver stage, v
ΔE	d-c thermocouple input, v
e_1	instantaneous voltage input to driver stage, v
e_g	instantaneous grid to cathode voltage of driver stage, v
f	frequency, cps
f_+	frequency with positive input, cps

f_- frequency with negative input, cps

f_o resonant frequency, or frequency with zero input, cps

Δf frequency deviation or change, cps

G galvanometer

g acceleration due to gravity, ft/sec^2

I_c peak-to-peak alternating current through tank capacitor, amp

I_o peak-to-peak fundamental component of shorted tank current due to diode mismatch, amp

ΔI average or direct current through thermocouple input (due to ΔE), amp

i_d instantaneous diode current, amp

i_o instantaneous current through tank due to thermocouple input, amp

i_{os} instantaneous shorted tank current, amp

j complex operator, $\sqrt{-1}$

L inductance of tank coil, h

L_u unbalancing inductance, h

Q ratio of inductive reactance to resistance in tank coil

R bridge resistance, ohms

R_1 plate and cathode load resistances in driver stage, ohms

R_d nominal diode resistance, ohms

R_k cathode resistance of first stage, ohms

R_L plate load resistance of first stage, ohms

R_o series resistances in driver stage, ohms

R_s series resistance in diode measuring circuit, ohms

R_u unbalancing resistance across diodes, ohms

ΔR_1 diode resistance change from 100° F at 1.0 ma to 220° F at 0.8 ma

ΔR_2 diode resistance change from 100° F at 0.85 ma to 220° F at 0.7 ma

ΔR_3 diode resistance change from 100° F at 0.45 ma to 220° F at 0.35 ma

ΔR_4 diode resistance change from 1.0 ma to 0.85 ma at 100° F

ΔR_5 diode resistance change from 1.0 ma to 0.45 ma at 100° F

ΔR_d nominal difference in resistance between upper and lower diode, ohms

r_d instantaneous diode resistance, ohms

$r_{d,av}$ average diode resistance, ohms

r_p driver-tube plate resistance, ohms

Δr_d instantaneous difference between top and bottom diode resistance, ohms

t time, sec

V_1 peak-to-peak a-c voltage across bottom diode, v

V_2 peak-to-peak a-c voltage across unbalancing inductance, v

V_3 peak-to-peak a-c voltage across bottom diode to ground, v

V_b peak-to-peak a-c voltage output from bridge (open circuit), v

V_c peak-to-peak a-c voltage across tank capacitor, v

V_d one-half total peak-to-peak a-c voltage across diode bridge, v

V_o overshoot peak voltage in capacitance-matching test, v

ΔV peak-to-peak a-c fundamental component of square wave due to inverting thermocouple input, v

v_c instantaneous voltage across tank capacitor, v

v_d one-half instantaneous voltage across diode bridge, v

v_k instantaneous cathode voltage of driver stage, v

δ certain small value which integrand of expression for I_o shall not exceed

θ phase angle (in a-c cycle), deg

φ_A amplifier phase shift, deg

φ_B diode-bridge phase shift (open circuit), deg

φ_T tank phase shift, deg

μ amplification factor of driver tube

ω angular velocity, radians/sec

ω_o resonant angular velocity, radians/sec

DISCUSSION OF PROBLEM

In order to arrive at the optimum design of a complete thermocouple telemeter, all the general methods of telemetering would have to be investigated. However, since it is desirable that the telemeter fit into the NACA telemetering system, advantage can be taken of the fact that this system has already been designed and used successfully for the past several years. It is similar in principle to the standard Research and Development Board (RDB) system (ref. 4) but differs in many details. A description of the NACA telemetering system is given in the following section.

Description of NACA Telemetering System

In the NACA telemetering system, a pickup instrument controls the frequency of a subcarrier oscillator. Several such oscillators, operating in different frequency bands or channels, between 100 and 200 kilocycles, simultaneously amplitude-modulate a 219.45-megacycle carrier frequency which is transmitted from the missile to the ground receiving station. At the ground station, the subcarrier frequencies are separated and fed into individual discriminators which produce a direct current proportional to the frequency deviation of the corresponding subcarrier oscillator. The direct currents are recorded on multichannel oscillographs. A block diagram of the system is shown in figure 1.

Subcarriers.- A maximum of 10 subcarriers spaced approximately 10 kilocycles apart are available, each having a nominal 3-kilocycle full-scale frequency deviation. The subcarrier oscillator in the missile is usually a two-tube oscillator with an inductance pickup (pickup inductance varies with quantity to be telemetered) in the parallel tank circuit. The volume of the oscillator is 5 cubic inches.

In the ground equipment, each subcarrier signal is heterodyned to a frequency band of 3 ± 1.5 kilocycles and thus the discriminators for the various channels are identical. The discriminator voltage output as a function of frequency input is linear within one-half of 1 percent.

Commutation of subcarrier channels.- In order to expand the capacity of the system, a commutator switch is used to sample several pickups on one or more subcarrier channels. The switch has a 30-position double-pole commutator and a speed of 5 rps. Inasmuch as two adjacent contacts are usually connected together, a sampling rate of 75 samples per second is obtained. The volume of the switch is about 17 cubic inches.

Frequency response.- The frequency response of the system is usually limited by the recorder galvanometer, which normally uses elements having a natural frequency of 100 cps. With commutated signals, a higher frequency response is required and 300 cps elements are used. With properly damped galvanometers, the transient response to a step function is completely damped in 1/180 of a second. Hence, a sampling rate of 90 samples per second gives very accurate data during the last half of each sample.

Measurement of new quantities.- The NACA telemetering system has become standardized to the extent that the measurement of any new quantity, such as an electromotive force, requires the design of a new subcarrier oscillator which will convert the desired quantity to a frequency-modulated signal.

Requirements of Thermocouple Oscillator

The problem has thus been narrowed down to that of designing a subcarrier oscillator which will produce the proper frequency deviation from a thermocouple electromotive force and be compatible with the NACA telemetering system. Other requirements of the oscillator are discussed in the following sections.

Temperature range and accuracy.- The maximum temperature range to be telemetered is from approximately 0° F to 2,000° F, although higher temperatures are foreseen in the near future. Thus, with a chromel-alumel couple, an output of 40 millivolts, or more, is obtained. Many applications call for ranges in the order of 0° F to 500° F, for which iron-constantan couples give a 15-millivolt output. The accuracy required is generally within 1 percent of full scale.

Size.- The instrumentation must be kept as small as possible to permit maximum performance of the missile; also, it is desirable to survey several temperatures along skin surfaces. In order to save space, the temperature pickups should be commutated. The use of commutation enables a smaller, less stable oscillator to be used because reference or calibration voltages can be sampled during flight to give good accuracy.

Stability.- It is desirable that the oscillator frequency be stable with changes in supply voltages and with temperature. However, since inflight calibration is used, some instability can be tolerated, provided the subcarrier frequency always stays within the 3-kilocycle channel band width. If the nominal full-scale deviation is reduced to 2 kilocycles, then the maximum allowable zero drift under all operating conditions can be 1 kilocycle or 50 percent of full scale.

Oscillator temperature.- Although skin temperatures during flight may reach 2,000° F due to aerodynamic heating, missile interiors will not reach this temperature because of time lag. Since radiation from the skin can cause excessive temperatures in the telemeter, a metal radiation shield is mounted between the telemeter and skin; therefore, the telemeter temperature rise during flight is about 20° F. Before launching, heat generated in the telemeter raises the temperature of the subcarrier oscillators about 80° F above the ambient air temperatures. Thus, the actual temperature of the oscillator may range from about 120° F to 200° F.

Vibration and acceleration.- The telemeter must give accurate data under the high acceleration (of the order of 100g) caused by the thrust of the rocket motor. Also, vibration as high as 50g may be encountered during the burning of the rocket propellant.

Frequency response.- The frequency response of the system must be adequate to handle a sampling rate of at least 75 samples per second; thus, the response of the system is required to be flat to about 200 cps.

Input resistance.- The input resistance of the oscillator at the thermocouple input terminals must be relatively high. Any current drawn by the telemeter will cause a voltage drop in the thermocouple lead wires and will produce an error if the pickup resistances are not equal to the calibration-source resistance. Pickup and lead resistance cannot be made exactly equal to that of the calibration source because lead wires become heated to unknown temperatures during flight. If pickup leads are within 10 ohms of the calibration source, then an input resistance in excess of 5,000 ohms is acceptable since an error of 0.2 percent is considered negligible.

One other important requirement for the input is that it be balanced to ground. Thermocouples are grounded to the skin at the junctions and cannot be grounded elsewhere.

Linearity.- Since the number of calibration points should be kept to a minimum, it is desirable to have a linear curve of frequency as a function of input, in which case zero- and full-scale points define the calibration. However, if this linearity cannot be achieved, a three-point calibration (zero-, half-, and full-scale) may be satisfactory.

Cold junction.- The thermocouple reference junction temperature must be known. The flight time is usually so short (of the order of 5 minutes) that a reasonably well insulated cold junction with some thermal inertia will keep a constant temperature throughout the useful flight.

Conversion of Thermocouple Electromotive Force to a Frequency-Modulated Signal

Most methods of converting thermocouple electromotive force to a frequency-modulated signal are inadequate for this application. Saturable reactors have low input resistance, high input inductance, and hysteresis. Voltage oscillators using vacuum-tube reactance modulators require preamplification of the signal by using either a d-c amplifier or an a-c amplifier with an inverter. Amplifiers using tubes have excessive microphonics and such a system would require too much space. (The possibility of using transistors was not investigated because, at the beginning of the present investigation, transistors were in their infancy.)

The method to be described in this report uses a diode bridge to invert the thermocouple electromotive force at a high frequency in conjunction with a phase-shift oscillator. This produces a compact unit free from the inadequacies just mentioned.

DIODE-BRIDGE—PHASE-SHIFT OSCILLATOR

The principle of operation of the subcarrier oscillator is best described by a simplified analysis which gives general design trends.

Phase-Shift-Oscillator Operation

A block diagram of the basic phase-shift oscillator is shown in figure 2(a) and the schematic diagram is shown in figure 2(b). The condition for oscillation is that the open-loop feedback voltage be in phase with (and greater than) the input to the amplifier. The phase shift through the amplifier φ_A is effectively zero. The phase shift through the tank circuit φ_T is -90° at resonance and varies with frequency. If the phase shift through the diode bridge φ_B is 90° and can be made to vary with thermocouple input voltage, then the frequency will vary about the resonant point according to the relation

$$\varphi_A + \varphi_B + \varphi_T = 0 \tag{1}$$

Diode-Bridge Operation

The diode-bridge circuit is shown in figure 3(a). The input (assumed sinusoidal) to the bridge, coming from the amplifier, is balanced with respect to ground, but the output of the bridge is single-ended. The thermocouple input is represented by the battery ΔE (one side grounded for simplicity).

Diode inverting action.- For the positive half-cycle of the bridge voltage $2V_d$ (fig. 3(a)), the diodes on the left are conducting with some forward resistance R_d (assumed constant throughout the half-cycle) but the diodes on the right are nonconducting. For matched diodes, the bridge is balanced and the voltage from point B to ground is zero. (For the moment, the capacitor C_u and the inductor L_u will be neglected.)

For the negative half-cycle, the diodes on the left are nonconducting, the voltage from point A to point B is zero, and the output voltage V_b is $-\Delta E$. Thus, it is seen that, for ideal diodes, the diode bridge actually operates as a high-frequency inverter. The output voltage at point B is a square wave with amplitude (peak-to-peak) ΔE, the thermocouple input voltage, and is in phase with the sine-wave input to the bridge. This operation is shown in the form of an equivalent circuit in figure 3(b), where R_d is the forward resistance of the diodes and ΔV is the peak-to-peak fundamental component of the square wave. Only the fundamental component

is important because of the resonant tank circuit which follows. (The amplitude of ΔV is approximately equal to ΔE.)

Bridge phase shift.- The effect of a small unbalancing capacitance C_u (and inductance L_u having an equal reactance) will now be considered. Since ΔV is small in comparison with V_1, the capacitance C_u can be assumed to be across V_1. In the vector diagram of figure 3(c), the voltage across the bottom diode V_1 is slightly lagging $2V_d$ with an amplitude nearly equal to V_d. The voltage V_3 is the sum of V_1 and the equivalent a-c thermocouple voltage ΔV, which is in phase with $2V_d$. The voltage V_2 is nearly equal to V_d in amplitude but is slightly leading in phase because of the unbalancing inductance L_u. The voltage V_b is the difference between V_2 and V_3, and it is seen that the phase depends upon the thermocouple voltage and varies around 90°.

Appendix A shows that the phase shift of the bridge is

$$\varphi_B \approx \tan^{-1} \frac{\omega C_u (R + R_d)}{2 \frac{\Delta V}{V_d} - \frac{\Delta R_d}{R_d}} \tag{2}$$

It should be emphasized that the voltage V_b is the open-circuit bridge output voltage. When the bridge is connected to the series resonant tank circuit, this output voltage is practically shorted to ground (if the frequency is near resonance) and V_1 is very nearly equal to V_2. Thus, C_u and L_u are essentially in parallel, and, if their values are adjusted to give parallel resonance, $2V_d$ will be approximately in phase with the driving voltage of the preceding amplifier and will give zero phase shift for that part of the amplifier even though R_d may change. For this reason, both C_u and L_u are used.

Frequency-Deviation Relation

Appendix B shows that the phase shift in the tank circuit is (when taking into account the output impedance of the bridge)

$$\varphi_T \approx \tan^{-1} \frac{f}{\Delta f} \frac{R + R_d}{4\omega L} \tag{3}$$

where Δf is the frequency deviation from resonance.

Equating the total phase shift to zero (assuming $\varphi_A = 0$) and solving for $\frac{\Delta f}{f}$ (appendix C) gives the approximate relation

$$\frac{\Delta f}{f} \approx \left(\frac{\Delta R_d}{4R_d} - \frac{\Delta V}{2V_d}\right)\frac{L_u}{L} \tag{4}$$

This relation shows that the sensitivity or frequency deviation for a given thermocouple input is proportional to L_u/L and inversely proportional to the voltage across the diode.

Equation (4) shows that a frequency change (zero shift) occurs if the diode mismatch $\Delta R_d/R_d$ changes. This effect is extremely important but undesirable. The diode mismatch can vary because of changes in temperature and V_d. The selection of diodes to reduce this zero shift is the major problem in the design of the oscillator and is described later.

Input Resistance

The input resistance can be defined as the d-c impedance presented to the thermocouple pickup at the input terminals; the resistance is equal to the ratio $\Delta E/\Delta I$, where ΔI is the average current drawn from ΔE. Other currents which flow through ΔE, but not caused by ΔE, are also important since they produce undesirable voltage drops in the thermocouple leads. It can be seen in figure 3(a) that the only current flowing through ΔE occurs during the negative half-cycle of V_d. Figure 3(b) applies because only the average current through ΔV during the negative half-cycle of V_d contributes to ΔI.

In figure 3(b) all the tank current in the negative half-cycle flows through ΔV and must be 90° out of phase with V_d (as shown in fig. 3(c), I_c must lead V_d by 90° and V_c must be in phase with V_d if the amplifier phase shift is zero); hence, the average current through ΔV is zero. This fact is based on the assumption that R_1 shown in figure 4(a) is high.

The bridge-driver circuit and its equivalent are shown in figure 4. The current drawn from ΔV is approximately $\frac{2\Delta V}{R_1 + R_o + r_{d,av}}$ (for one-half cycle); hence, the input resistance is $R_1 + R_o + r_{d,av}$.

DIODE SELECTION

Equation (4) showed that the oscillator frequency is not only a function of thermocouple input but also of diode mismatch. It can be seen from figure 3(b) that a mismatch of diode impedance during any part of either half-cycle will produce a voltage output from the bridge indistinguishable from the thermocouple input. This mismatch therefore should be kept as small as possible. In the following sections, a method for matching diodes is discussed.

Diode Characteristics

Diode forward resistance, in general, varies widely with applied voltage, with temperature, and from one diode to another. Silicon-junction diodes have much better temperature characteristics than other available diodes. They not only change less with temperature variations but can also withstand a higher temperature without permanent damage and have less variation from diode to diode. A typical plot of forward resistance against current at three temperatures is shown in figure 5. The rated maximum diode temperature is 150° C (302° F). At a current of about 6 ma, the resistance of the diodes does not change with temperature, and operating the diodes near this region would seem desirable; however, it is difficult to drive them at this high current, and the recovery time (which shows up as a large effective capacitance at 100 kilocycles) is too great. (New diodes with very little capacitance are now becoming available and should be more desirable.) It was found that these silicon-junction diodes could be used at the lowest three frequency channels (110 to 130 kilocycles) with peak currents of 1 ma provided that they are matched for capacitance as well as resistance.

Diode-Resistance-Matching Analysis

It may be surmised that diodes must be matched closest near the peak of the a-c cycle for the following reasons:

(1) Only the fundamental component of the bridge output is important (series tank circuit filters out harmonics); hence, output due to diode mismatch near the zero part of the cycle contributes little to this fundamental component.

(2) Limiting flattens the voltage peak across the diodes and causes the diodes to operate near this condition for a large part of the cycle.

(3) Near the zero part of the cycle, the diode resistance is high; hence, unbalance is ineffective in producing an output since fixed resistors R shunt the diodes.

Appendix D shows that, in order to keep the effective instantaneous mismatch below a certain level throughout the cycle, the allowable mismatch Δr_d (normalized at the peak of the cycle) should be less than that shown in figure 6. Since it is practical to match diodes only at a limited number of current values (say three), then it is logical that the values be equally spaced timewise throughout the cycle. A plot of diode current i_d against phase angle θ (calculated by using formulas in appendix D) is shown in figure 7. No appreciable current flows through the diodes until a phase angle of 27° is reached; hence, matching is important only between 27° and 90°. Thus, the values of current were chosen at approximately 47°, 68°, and 90°. The values of current chosen and the corresponding values of Δr_d allowed are as follows:

i_d, ma	$(\Delta r_d)_{relative}$	$(\Delta r_d)_{actual}$, ohms
1.00	1.0	1
.85	1.5	2
.45	4.0	4

Diode-Resistance Measurements

Experience shows that a practical method of selecting matched pairs of diodes is to make resistance measurements on a large group (over 100), and then select the best matched pairs. Measurements are made at 100° F for 1.0, 0.85, and 0.45 ma and at 220° F for 0.8, 0.7, and 0.35 ma. Lower currents are used at the higher temperature because the diode voltage in an oscillator is reduced when the diodes are heated; therefore, the resistance at the peak of the cycle is made approximately the same for all temperatures. In order to aid in matching, a resistor may be inserted in series with any diode in the final bridge. Hence, all diode resistances are measured at a specific current (rather than a specific voltage) so that the total resistance at that specific current is always the sum of the diode resistance and the series resistance.

The circuit for measuring the resistance is shown in figure 8. Diodes are placed in a temperature-regulated oven. Current is kept at the desired value by adjusting R_s. Since a resistor may be inserted in series with one diode of a pair in order to match at the 1.0-ma, 100° F condition, only the resistance changes from this condition are important in matching. Therefore, the following resistance changes are calculated for each diode: ΔR_1, ΔR_2, ΔR_3, ΔR_4, and ΔR_5.

Capacitance Matching

The capacitance is not measured directly. Figure 9 shows the circuit used for determining relative capacitance effects. The diodes are kept at room temperature. The overshoot voltage V_o is measured for each diode with an oscilloscope. The maximum variation in V_o is about 0.7 volt. Pairs are arbitrarily matched within ±0.05 volt.

Selection of Diode Pairs

The resistance changes calculated are arranged in order of decreasing value of ΔR_1. Table I shows part of the data obtained in a group of diodes. The tolerances allowed are shown at the bottom of each column. The following are the matched diode pairs chosen from this table:

$$\begin{Bmatrix} 903 \\ 1001 \end{Bmatrix} \text{ and } \begin{Bmatrix} 927 \\ 970 \end{Bmatrix}$$

From a group of 300 diodes, 40 pairs can usually be matched within the specified tolerances.

OSCILLATOR DESIGN, CONSTRUCTION, AND OPERATING PROCEDURE

Electrical Circuit

A schematic diagram of the complete oscillator is shown in figure 10. The first stage is the amplifier, the second stage is the bridge driver, and the third stage is the output.

First stage.- The gain of the first stage is adjusted with the plate and cathode resistors. Stable resistors (such as precision molded-boron-carbon type) are required. The cathode capacitor compensates for the phase shift caused by capacitance to ground between the first and second stage and gives nearly zero phase shift for the amplifier.

Second stage.- The second stage is a phase inverter which provides a balanced output for driving the diode bridge. The plate and cathode load resistors must be matched, and stable resistors (molded-boron-carbon type) are used. The coupling capacitors between the second stage and the bridge are relatively small in order to filter out low-frequency microphonics generated in the first stage, and they are matched.

Limiting: Limiting in the oscillator occurs in the diode bridge because of nonlinearity of the diodes and tends to keep a constant (peak) voltage across the diodes. If the gain of the amplifier should change, the current through the diodes changes but the diode (peak) voltage remains essentially constant. This limiting action flattens the voltage wave shape across the diodes and makes the diodes operate within a small range of resistance for a large part of the cycle; thus, the diodes may be matched over a small range. Limiting improves frequency—supply-voltage stability by keeping the diode voltage constant and also gives a more linear frequency as a function of thermocouple input because a change in thermocouple input changes the voltage across the tank capacitor C. Without limiting, the voltage across the diodes V_d would change and thereby cause a change in sensitivity and nonlinearity. Diodes do not limit properly if driven from a very low impedance source (such as a cathode follower); hence, the resistors R_o (matched molded-boron-carbon type) are necessary.

Bridge circuit: The grounded capacitors across the thermocouple input terminals provide an a-c ground for the bridge but keep the thermocouple input insulated from ground; thus, a balanced input to ground is provided. A large value is used so that changes in thermocouple resistance will not affect the a-c impedance; nevertheless, the capacitance must be small enough to give good frequency response with normal pickup resistance.

The inductor L_u is universally wound on a small powdered iron core and tapped to provide sensitivities ranging from 10 to 45 millivolts (full scale). Only three taps are necessary because the effective reactance may be finely adjusted by another capacitor C_u' in parallel with the inductor L_u. Capacitor C_u plus C_u' should give parallel resonance with L_u. The resistors R (molded-boron-carbon type) must be matched to a high degree.

Tank circuit: The inductance L in the tank circuit is 1.5 mh which gives the proper range of sensitivities and also keeps capacitance C high to reduce effects of input capacitance of the first stage. The inductor is an air-core universally-wound type with a good temperature coefficient.

Third stage.- The third or output stage (cathode follower) isolates the output and is desirable to prevent loading by other oscillators connected to the common output. The output stage takes its voltage from the cathode of the driver tube where a good sine wave and a low impedance exists.

Construction of Oscillator

The oscillator uses small component parts and occupies very little space (volume of approximately 10 cubic inches). Figure 11 is a photograph of all the electrical components which go into the oscillator. Figure 12 is a photograph of a complete oscillator with standard shield can and cover.

The chassis is molded glass-fiber-filled phenolic and the interior is potted with Paraplex to give good mechanical rigidity.

A copper shield is mounted around the diode bridge in order to prevent temperature gradients between the matched diodes. Care is taken to keep the bridge away from heat sources, such as the plate or cathode resistors of the last two stages.

Several terminals (indicated in fig. 10 by circles) are provided to allow external mounting of parts which must be adjusted. Most adjustments are made by selecting and soldering in fixed components. Once these components are chosen, they need not be changed. This procedure gives good mechanical stability.

Adjustments which are continuously variable are center frequency with the 7 to 45 μμf trimmer capacitor (a part of C) and the output voltage with the 500,000-ohm miniature variable resistor. Easy adjustment is required to adjust all subcarriers for equal modulation of the carrier.

Operational Adjustments of Oscillator

Adjustments of the oscillator are quite critical for obtaining good operation. The following is a brief procedure.

Capacitor C is adjusted by connecting a low-impedance generator from point B (fig. 10) to ground and tuning capacitor C for series resonance at the center frequency of the subcarrier. Next, L_u, C_u, and C_u' (values to give proper sensitivity may at first be obtained by trial and error) are connected in parallel and tuned to parallel resonance at center frequency by use of a high-impedance generator, and then they are connected properly in the circuit. The resistor R_k is adjusted to give the desired peak-to-peak voltage (at 120° F) across the diodes (that is, across C_u) with the oscillator operating. Finally, C_k is adjusted to give oscillation at center frequency and then R_k, or R_L, is readjusted to give proper voltage across C_u. A microammeter is connected in series with the thermocouple input voltage source and should read zero. In some cases, a resistor R_u across one side of the diode bridge to ground is necessary to give zero current.

Sometimes it is necessary to bypass (at the chassis terminals) all external connections in order to prevent radio frequency (219.45-megacycle carrier) from entering the oscillator.

Pickup, Calibration, and Switch Circuit

Figure 13 shows a sample schematic diagram of the pickup, calibration, and switch circuit. The calibration network provides zero-, half-, and full-scale references. Each one has a balanced resistance of 50 ohms to ground. A nickel-wire resistance pickup is connected so as to telemeter cold-junction temperatures if necessary.

Resistors are connected in series with each thermocouple in order to give approximately 50 ohms to ground on all leads. (Pickup leads are not usually the same length.)

PERFORMANCE TESTS OF OSCILLATOR UNITS

The following sections give results of performance tests made on seven of the first oscillator units constructed. Although these units did not incorporate all of the latest improvements, they do show that the oscillator meets the requirements mentioned previously. (A limited investigation of the newest oscillator units has shown that temperature stability, warmup drift, input resistance, and linearity have been improved.)

The oscillators in the tests were adjusted for about 20 millivolts (full scale) and tested with a ±10-millivolt source. In general, performance is better for lower sensitivities than for higher sensitivities. Adjustments were made with the oscillator at 120° F. Table II gives the values of the adjustable components.

Warmup Drift

Figure 14 shows a plot of frequency against time during warmup of the oscillators. (Oscillators were allowed to cool after the adjustments mentioned in the previous paragraph were made.) A period of 30 minutes is needed for the frequency to stabilize. Temperature measurements were made with a mercury thermometer inserted inside the shield cover.

Subsequent tests were made under steady-state temperatures. The oscillators were cooled or heated externally to obtain the temperature range of 100° F to 200° F.

Stability

Figure 15 shows a plot of zero-input frequency drift against temperature. The range tested is beyond that expected under actual flight conditions. The greatest change is 0.5 kilocycle over the probable operating range of 120° F to 200° F.

Figure 16 shows how the sensitivity varies with temperature. (No attempt was made to adjust all oscillators to exactly the same sensitivity.) The variation in sensitivity is about 20 percent over the range 120° F to 200° F. This change is undesirable but is acceptable since inflight calibration will eliminate this source of errors. Figure 17 shows the diode voltage (as measured with a vacuum-tube voltmeter) against temperature. A reading of 0.5 volt represents a peak-to-peak voltage of approximately 1.4 volts. This change in voltage causes the sensitivity to change.

Figure 18 shows the change in zero-input frequency for a B^+ change from 150 to 180 volts and an A^+ change from 6 to 7 volts. The sensitivity changed an average of 1.5 percent of full scale for B^+ and 0.8 percent of full scale for A^+ changes.

Linearity

Linearity of frequency as a function of input was determined by measuring the oscillator frequencies at inputs of -10, 0, and 10 millivolts - designated herein as the frequencies f_-, f_o, and f_+, respectively. A straight-line calibration between end points would give the frequency $\frac{f_+ + f_-}{2}$ for zero input. Hence, the deviation from a straight line is $f_o - \frac{f_+ + f_-}{2}$. This deviation is the maximum for a calibration with nearly constant curvature, as is the case here. The linearity did not vary appreciably with the aforementioned B^+ and A^+ changes. Figure 19 shows very little variation of linearity with temperature but does show some differences between oscillators. The maximum deviation from a straight line was approximately 0.5 percent and the average deviation was approximately 0.3 percent.

Input Resistance

The input resistance was measured by observing the current change caused by a 20-millivolt input change. The average input resistance for all units (under all conditions) was 9,500 ohms.

One quantity which is as important as input resistance is the current through the pickup with zero voltage input. Figure 20 shows the pickup

current as a function of temperature and the changes which occurred for a 30-volt change in B^+ and a 1-volt change in A^+. The maximum current under all conditions of test (including 10-millivolt input) was about ±4 microamperes. Thus, if the pickup resistance differs from the calibration by as much as 10 ohms, the maximum error is ±40 microvolts, or ±0.2 percent of full scale.

Vibration and Acceleration Tests

Each oscillator was tested with a 75g drop in the two directions perpendicular to the tubes. (These are the worst directions.) Each unit was also vibrated in these two directions through a continuous range of frequencies between 100 and 500 cps with a constant acceleration of 20g, and the output was continuously recorded by using a discriminator and a 300-cycle galvanometer. (A few tests were made at 30g.) Table III gives the maximum peak-to-peak noise encountered in each test.

Flight Tests

Many oscillators have been used in flight to obtain useful temperature data. A sample of an actual flight record is shown in figure 21. Two channels are shown with 12 pickups on each channel.

CONCLUDING REMARKS

The thermocouple subcarrier oscillator meets all of the requirements necessary for satisfactorily telemetering temperatures from pilotless aircraft. The linearity is such that two points establish the calibration within 0.5 percent, the input resistance is sufficiently high so that a 10-ohm difference between pickup and calibrate resistance causes negligible error, and the frequency response is well within the requirement to handle a sampling rate of 75 samples per second. The oscillator has a volume of 10 cubic inches, fits into the standard NACA telemeter chassis, and is compatible with the NACA telemetering system. The sensitivity can be adjusted to give 10 to 45 millivolts (full scale).

The stability tests show that if adjustments on the oscillator are made after a 30-minute warmup to give a 2-kilocycle full-scale frequency deviation, the frequency will stay within the 3-kilocycle discriminator band width under all conditions of operation.

With the use of inflight calibration, the system is capable of maintaining an overall accuracy within 1 or 2 percent of full scale. The

several hours of operation during testing, as well as the flights that have been made with these oscillators, show that they are operationally reliable.

Langley Aeronautical Laboratory,
National Advisory Committee for Aeronautics,
Langley Field, Va., August 14, 1957.

APPENDIX A

BRIDGE-CIRCUIT PHASE SHIFT

In determining the phase shift of the bridge circuit, it can be seen from figure 3(b) that

$$V_b = V_2 - V_3 = V_2 - V_1 + \Delta V \tag{A1}$$

In order to find the effect of a diode mismatch, in addition to the effect of thermocouple input, assume that the upper diodes differ in resistance by an amount ΔR_d. Then,

$$V_b = \frac{\dfrac{R\left(j\omega L_u\right)}{R + j\omega L_u}}{R + \dfrac{R\left(j\omega L_u\right)}{R + j\omega L_u}} 2V_d - \frac{\dfrac{\dfrac{R_d}{j\omega C_u}}{R_d + \dfrac{1}{j\omega C_u}}}{R_d - \Delta R_d + \dfrac{\dfrac{R_d}{j\omega C_u}}{R + \dfrac{1}{j\omega C_u}}} 2V_d + \Delta V \tag{A2}$$

Simplifying equation (A2) gives

$$\frac{V_b}{2V_d} = \frac{1}{2 + \dfrac{R}{j\omega L_u}} - \frac{1}{2 + j\omega C_u R_d - \dfrac{\Delta R_d}{R_d}\left(1 + j\omega C_u R_d\right)} + \frac{\Delta V}{2V_d} \tag{A3}$$

If C_u and L_u are assumed to have the same reactance and second-order terms $\left(\omega L_u = \dfrac{1}{\omega C_u} > R\right)$ are neglected, equation (A3) reduces to

$$\frac{V_b}{2V_d} \approx \frac{\Delta V}{2V_d} - \frac{1}{4}\frac{\Delta R_d}{R_d} + \frac{1}{4} j\omega C_u\left(R + R_d\right) \tag{A4}$$

Thus, the phase shift across the bridge is

$$\varphi_B \approx \tan^{-1} \frac{\omega C_u\left(R + R_d\right)}{2\,\frac{\Delta V}{V_d} - \frac{\Delta R_d}{R_d}} \tag{A5}$$

APPENDIX B

TANK-CIRCUIT PHASE SHIFT

If the output impedance of the bridge is assumed to be $\frac{R + R_d}{2}$, the output voltage of the tank circuit V_c across capacitor C (see fig. 2(b)) is

$$V_c = \frac{\frac{1}{j\omega C}}{\frac{R + R_d}{2} + j\omega L + \frac{1}{j\omega C}} V_b \tag{B1}$$

or

$$\frac{V_c}{V_b} = \frac{1}{\frac{R + R_d}{2} j\omega C - \omega^2 LC + 1} \tag{B2}$$

The phase shift through the tank circuit is then

$$\varphi_T = \tan^{-1} \frac{\omega C \frac{R + R_d}{2}}{\omega^2 LC - 1} \tag{B3}$$

Letting

$$\omega_o{}^2 = \frac{1}{LC} \tag{B4}$$

gives

$$\varphi_T = \tan^{-1} \frac{\frac{\omega}{\omega_o{}^2 L} \frac{R + R_d}{2}}{\frac{\omega^2}{\omega_o{}^2} - 1} \tag{B5}$$

but

$$\frac{\omega^2}{\omega_o{}^2} - 1 \approx \frac{2\,\Delta f}{f_o} \tag{B6}$$

where Δf is the change in frequency $\left(f - f_o\right)$. Therefore, since f is nearly equal to f_o,

$$\varphi_T \approx \tan^{-1} \frac{f}{\Delta f} \frac{R + R_d}{4\omega L} \tag{B7}$$

APPENDIX C

TOTAL PHASE SHIFT AND FREQUENCY EQUATION

Inasmuch as the phase shift in the amplifier is assumed to be zero, the total phase shift for oscillation is

$$\varphi_B + \varphi_T = 0 \tag{C1}$$

Substituting equations (A5) and (B7) into equation (C1) gives

$$\tan^{-1} \frac{\omega C_u\left(R + R_d\right)}{2\,\frac{\Delta V}{V_d} - \frac{\Delta R_d}{R_d}} + \tan^{-1} \frac{f}{\Delta f}\,\frac{R + R_d}{4\omega L} \approx 0 \tag{C2}$$

Simplifying equation (C2) gives the frequency equation

$$\frac{\Delta f}{f} \approx \frac{\frac{\Delta R_d}{4R_d} - \frac{\Delta V}{2V_d}}{\omega^2 L C_u} \tag{C3}$$

and, since

$$C_u = \frac{1}{\omega^2 L_u} \tag{C4}$$

equation (C3) reduces to

$$\frac{\Delta f}{f} \approx \left(\frac{\Delta R_d}{4R_d} - \frac{\Delta V}{2V_d}\right)\frac{L_u}{L} \tag{C5}$$

APPENDIX D

DIODE-RESISTANCE-MATCHING ANALYSIS

The following quantitative analysis derives an expression for the output caused by diode unbalance. From this expression, the allowable mismatch throughout the cycle is determined as a function of diode current.

Tank Current Caused by Diode Mismatch

The driver, bridge, and tank circuits are shown in figure 22(a). The equivalent circuit is shown in figure 22(b). It is desired to find the output voltage v_c, or current through C, which is caused by diode mismatch. As a general principle, the current i_o (fig. 22(b)) that will flow through a series resonant circuit driven by a periodic source (which has a fundamental near the resonant frequency) is the fundamental component of the short-circuit current i_{os} (fig. 22(c)). This rule applies only if the resonant circuit has a high Q or a low resistance in comparison with the source impedance. The approximation seems close enough for this purpose.

The equivalent circuit is shown in figure 22(c) with the tank shorted. If R_1 and r_p are high, then the instantaneous short-circuit output current is approximately

$$i_{os} \approx \frac{\frac{\Delta r_d}{r_d} v_d}{r_d + R} \tag{D1}$$

where v_d is one-half of the voltage across the diode bridge. Thus, the fundamental component of shorted tank current due to diode mismatch is

$$I_o = \frac{2}{\pi} \int_0^{\pi} i_{os} \sin \theta \, d\theta \tag{D2}$$

where $\theta = \omega t$.

In order to evaluate equation (D2), the value of $\sin \theta$ must be found. From figure 22(c), it may be seen that (Δr_d being neglected):

$$v_k \approx \frac{\dfrac{R_1\left(R_o + \dfrac{Rr_d}{R + r_d}\right)}{R_1 + R_o + \dfrac{Rr_d}{R + r_d}}}{r_p + 2\dfrac{R_1\left(R_o + \dfrac{Rr_d}{R + r_d}\right)}{R_1 + R_o + \dfrac{Rr_d}{R + r_d}}}\mu e_g \tag{D3}$$

From figure 22(a)

$$e_g = e_1 - v_k \tag{D4}$$

Substituting equation (D4) into equation (D3) and solving for v_k gives

$$v_k \approx \frac{e_1}{1 + \dfrac{2}{\mu} + \dfrac{r_p}{\mu}\dfrac{R_1 + R_o + \dfrac{Rr_d}{R + r_d}}{R_1\left(R_o + \dfrac{Rr_d}{R + r_d}\right)}} \tag{D5}$$

But, from figure 22(c),

$$v_d = \frac{\dfrac{Rr_d}{R + r_d}}{R_o + \dfrac{Rr_d}{R + r_d}} v_k \tag{D6}$$

Substituting equation (D5) into equation (D6) and simplifying gives

$$v_d \approx \frac{e_1}{\dfrac{R + r_d}{Rr_d}\left[R_o\left(1 + \dfrac{2}{\mu} + \dfrac{r_p}{R_1\mu}\right) + \dfrac{r_p}{\mu}\right] + 1 + \dfrac{2}{\mu} + \dfrac{r_p}{R_1\mu}} \tag{D7}$$

If R_1 and μ are high, then

$$v_d \approx \frac{e_1}{\frac{R + r_d}{Rr_d}\left(R_o + \frac{r_p}{\mu}\right) + 1} \tag{D8}$$

Since the voltage e_1 is sinusoidal with amplitude E_1,

$$e_1 = E_1 \sin \theta \tag{D9}$$

Thus, equation (D8) becomes

$$v_d \approx \frac{E_1 \sin \theta}{\frac{R + r_d}{Rr_d}\left(R_o + \frac{r_p}{\mu}\right) + 1} \tag{D10}$$

Hence,

$$\sin \theta \approx \frac{v_d}{E_1}\left[1 + \frac{R + r_d}{Rr_d}\left(R_o + \frac{r_p}{\mu}\right)\right] \tag{D11}$$

where

$$v_d = i_d r_d \tag{D12}$$

Thus, the fundamental component due to diode mismatch is as follows when equations (D1), (D11), and (D12) are substituted into equation (D2):

$$I_o = \frac{2}{\pi E_1 R} \int_0^{\pi} \Delta r_d i_d^2 \left(\frac{Rr_d}{R + r_d} + R_o + \frac{r_p}{\mu}\right) d\theta \tag{D13}$$

Diode Matching

Since two diodes cannot be made identical, the best method of choosing diode pairs would be to choose those which give a minimum value

of I_o. One way of doing this is to keep the integrand of equation (D13) always less than a certain small value δ for all values of θ (that is, throughout the half-cycle). Thus, make

$$\Delta r_d i_d^2\left(\frac{Rr_d}{R + r_d} + R_o + \frac{r_p}{\mu}\right) < \delta \tag{D14}$$

or

$$\Delta r_d < \frac{\delta}{i_d^2\left(\frac{Rr_d}{R + r_d} + R_o + \frac{r_p}{\mu}\right)} \tag{D15}$$

Normalizing so that the value of Δr_d is 1 at the peak current of 1 ma and substituting the values of circuit constants gives

$$(\Delta r_d)_{relative} = \frac{1158 \times 10^{-6}}{i_d^2\left(\frac{1000r_d}{1000 + r_d} + 750\right)} \tag{D16}$$

REFERENCES

1. McLarren, Robert: Guided Missile Friction Heating. Aero Digest, vol. 63, no. 2, Aug. 1951, pp. 27-30, 80-86.

2. Chauvin, Leo T., and deMoraes, Carlos A.: Correlation of Supersonic Convective Heat-Transfer Coefficients From Measurements of the Skin Temperature of a Parabolic Body of Revolution (NACA RM-10). NACA TN 3623, 1956. (Supersedes NACA RM L51A18.)

3. Fricke, Clifford L., and Smith, Francis B.: Skin-Temperature Telemeter for Determining Boundary-Layer Heat-Transfer Coefficients. NACA RM L50J17, 1951.

4. Nichols, Myron H., and Rauch, Lawrence L.: Radio Telemetry. Second ed., John Wiley & Sons, Inc., c.1956, pp. 417-428, 434-443.

TABLE I

PART OF MATCHING DATA OBTAINED ON A LARGE GROUP OF DIODES

Diode	ΔR_1, ohms	ΔR_2, ohms	ΔR_3, ohms	ΔR_4, ohms	ΔR_5, ohms	ΔV_o, v
903	5	33	24	107	723	0.19
927	5	31	16	107	726	.14
944	5	31	14	109	739	.13
949	5	31	17	109	736	.23
951	5	35	12	113	742	.69
960	5	31	22	109	734	.57
962	5	31	32	107	718	.29
970	5	32	18	107	725	.18
978	5	29	14	108	735	.63
1,001	5	31	23	106	723	.19
Tolerance	1 ohm	2 ohms	4 ohms	2 ohms	4 ohms	0.05 v

TABLE II

VALUES OF ADJUSTABLE COMPONENTS FOR SEVEN OSCILLATORS TESTED

[L_u = 3.5 mh]

Oscillator	R_L, ohms	R_k, ohms	C_k, μμf	C (external part), μμf (a)	C_u, μμf	C_u', μμf	R_u, ohms
1	27,000	1,500	360	390 + 110	430	82	------
2	30,000	1,300	300	553	430	82	33,000
3	25,000	1,500	300	470 + 110	430	82	------
4	27,000	1,300	300	430 + 110	430	82	------
5	27,000	1,400	390	470 + 110	390	82	39,000
6	30,000	1,200	510	470 + 110	430	82	------
7	22,000	1,500	240	430 + 110	470	82	------

[a] 110 μμf in C is N750 temperature-compensating capacitor.

TABLE III

MAXIMUM PEAK-TO-PEAK NOISE ENCOUNTERED DURING ACCELERATION

TESTS ON SEVEN OSCILLATORS

Oscillator	Noise in percent of full scale					
	Side acceleration			Top acceleration		
	75g drop	20g vibration	30g vibration	75g drop	20g vibration	30g vibration
1	3	2.5	11	5	4	---
2	1	---	1.5	1	---	3
3	1.5	1	----	1	2	---
4	1	2	4	1	1	---
5	1	1.5	----	.5	1	---
6	1	1	----	2	1	---
7	1	1	----	1.5	1.5	2.5

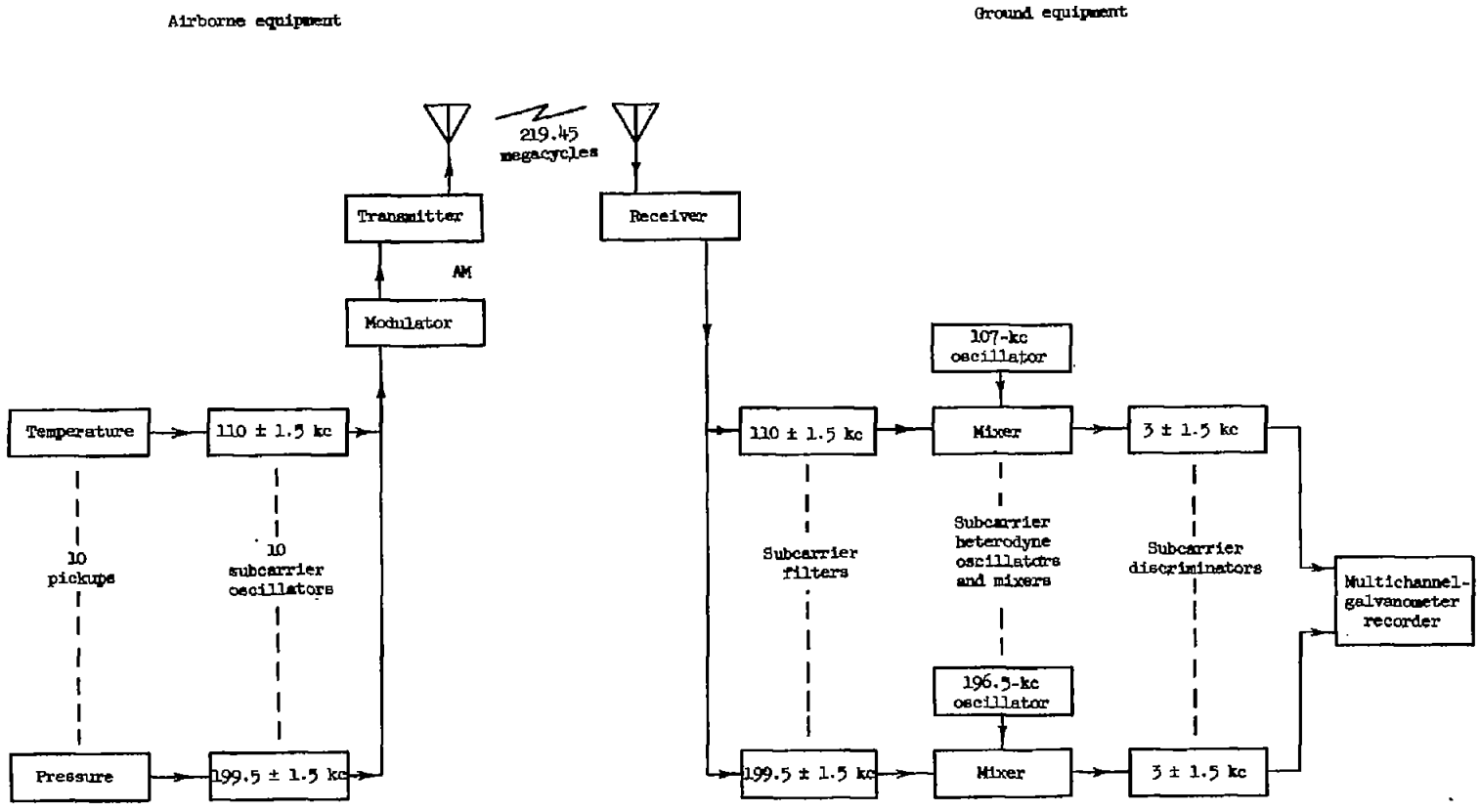

Figure 1.- Block diagram of NACA telemetering system.

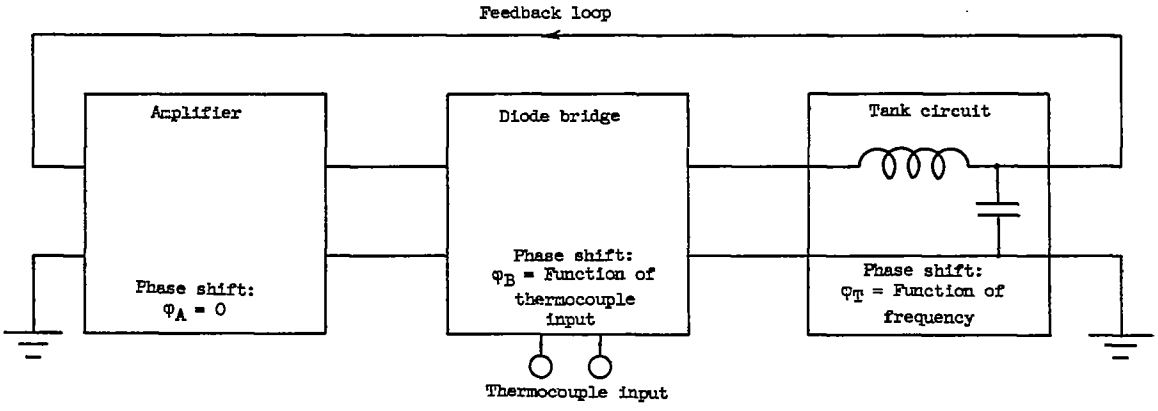

(a) Block diagram of basic oscillator.

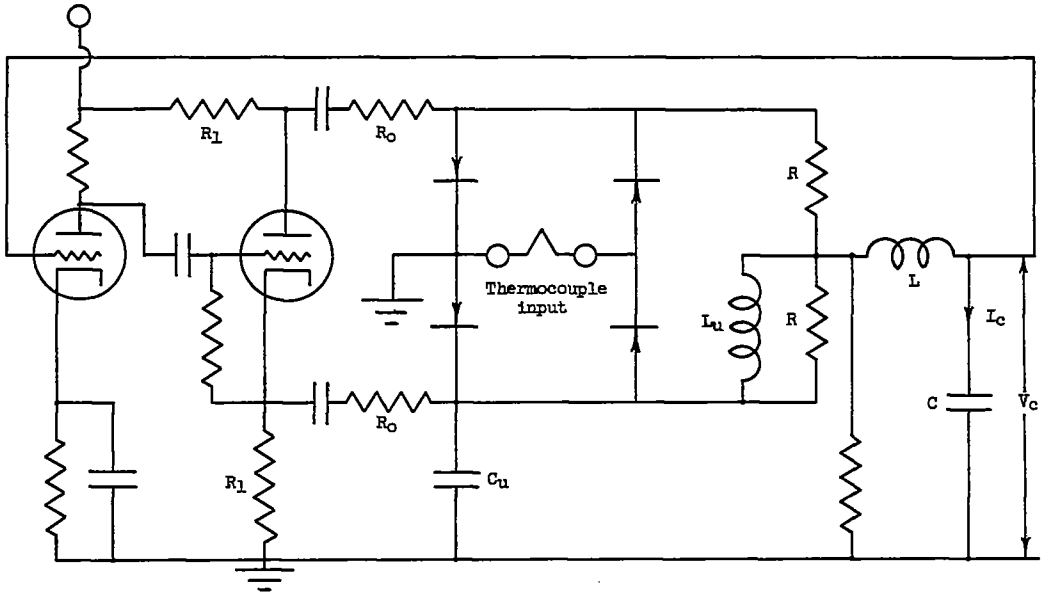

(b) Schematic diagram of basic oscillator.

Figure 2.- Phase-shift oscillator.

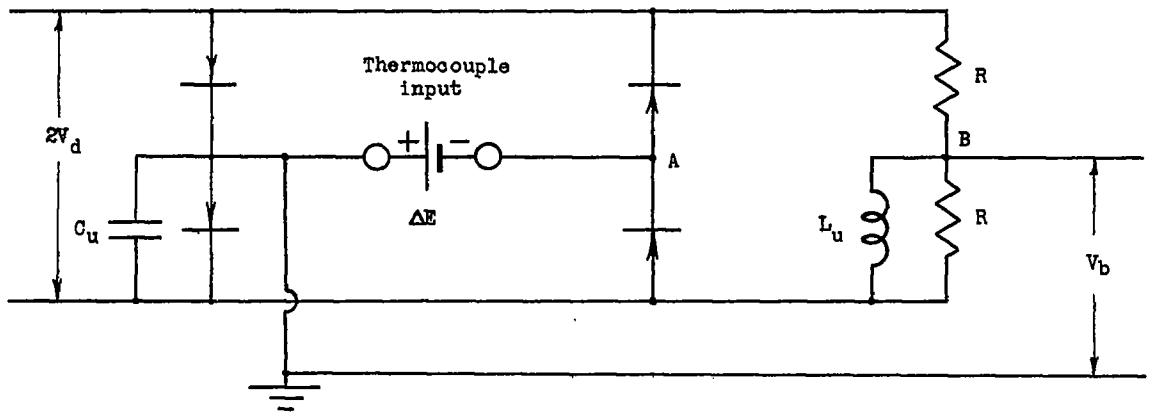

(a) Diode-bridge circuit.

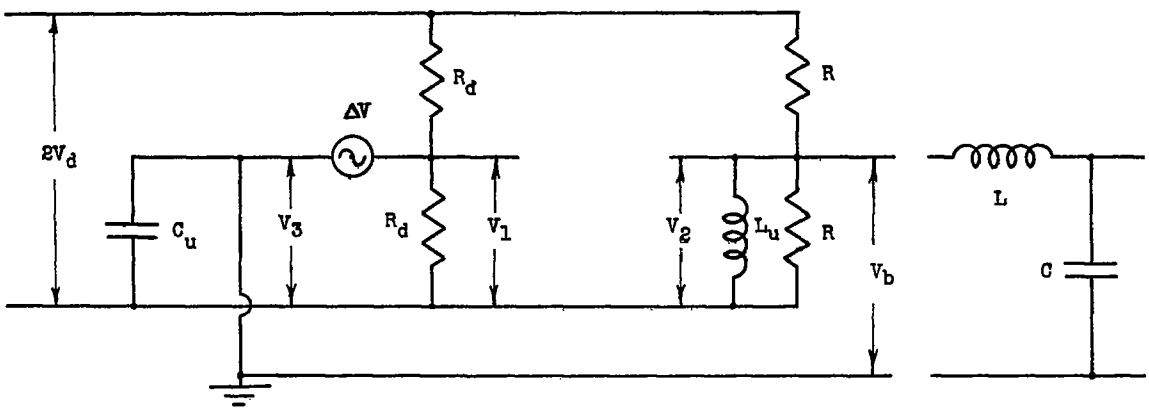

(b) Equivalent circuit.

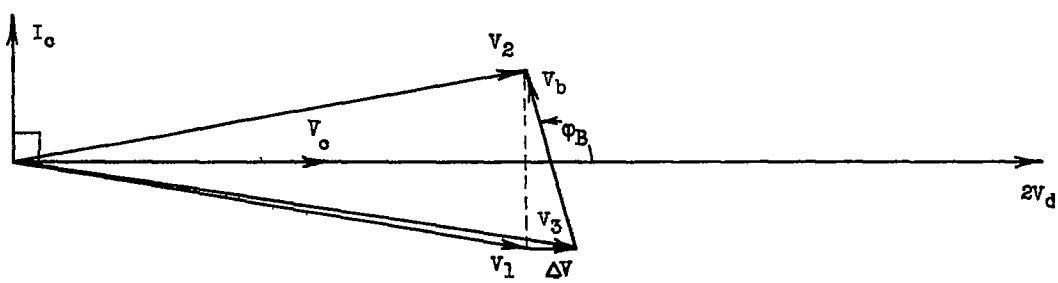

(c) Vector diagram.

Figure 3.- Diode-bridge diagrams.

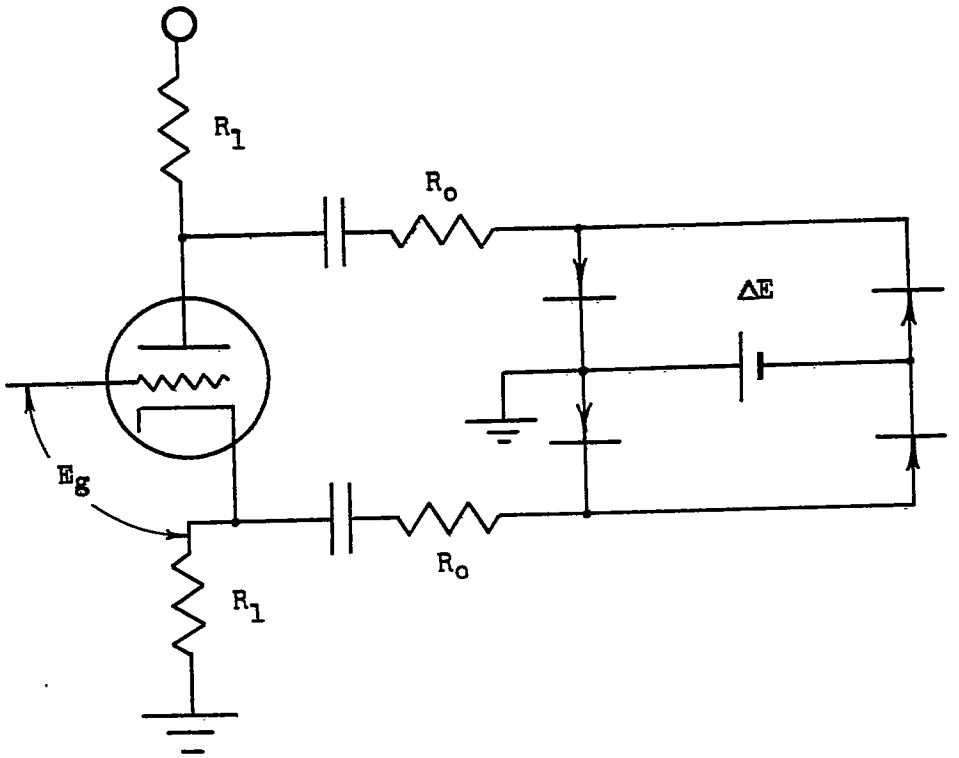

(a) Actual circuit.

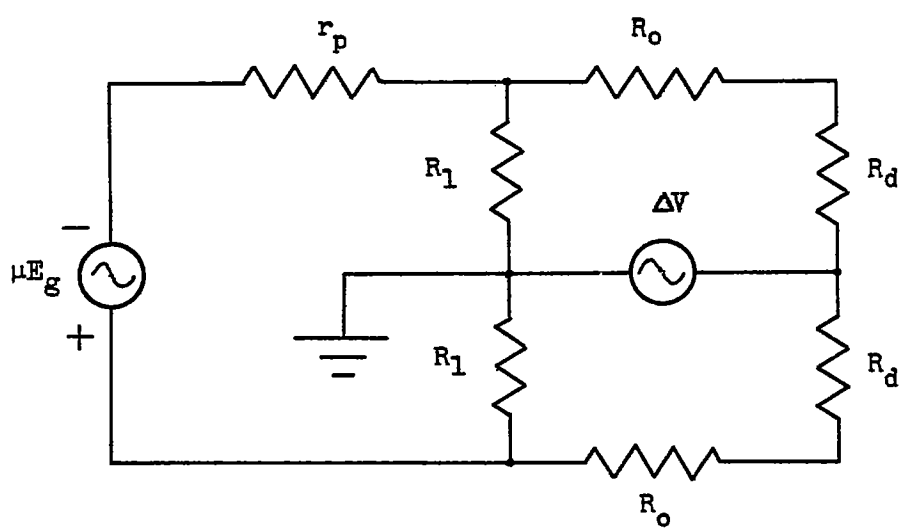

(b) Equivalent circuit.

Figure 4.- Bridge-driver circuit.

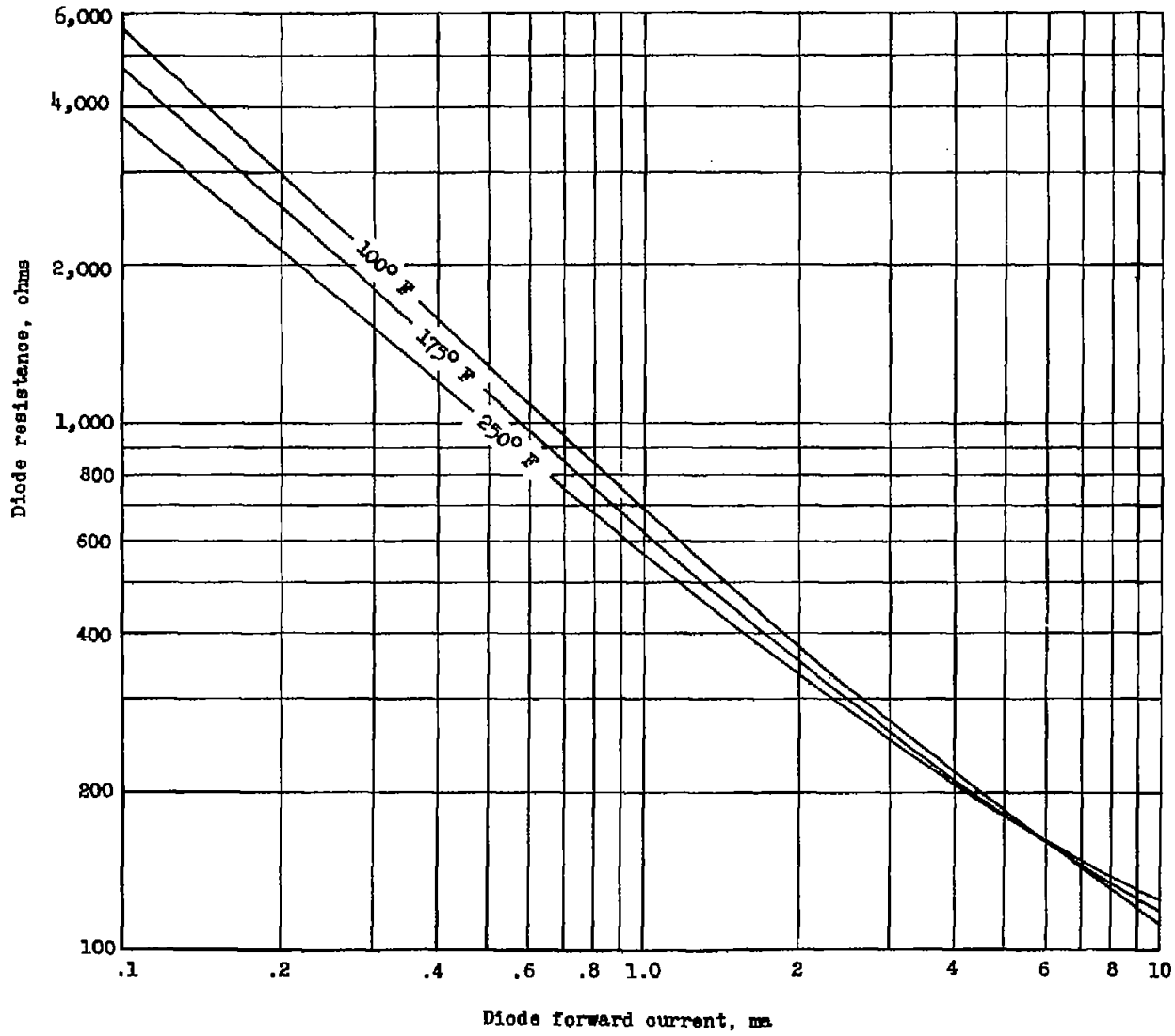

Figure 5.- Typical silicon-junction diode characteristics.

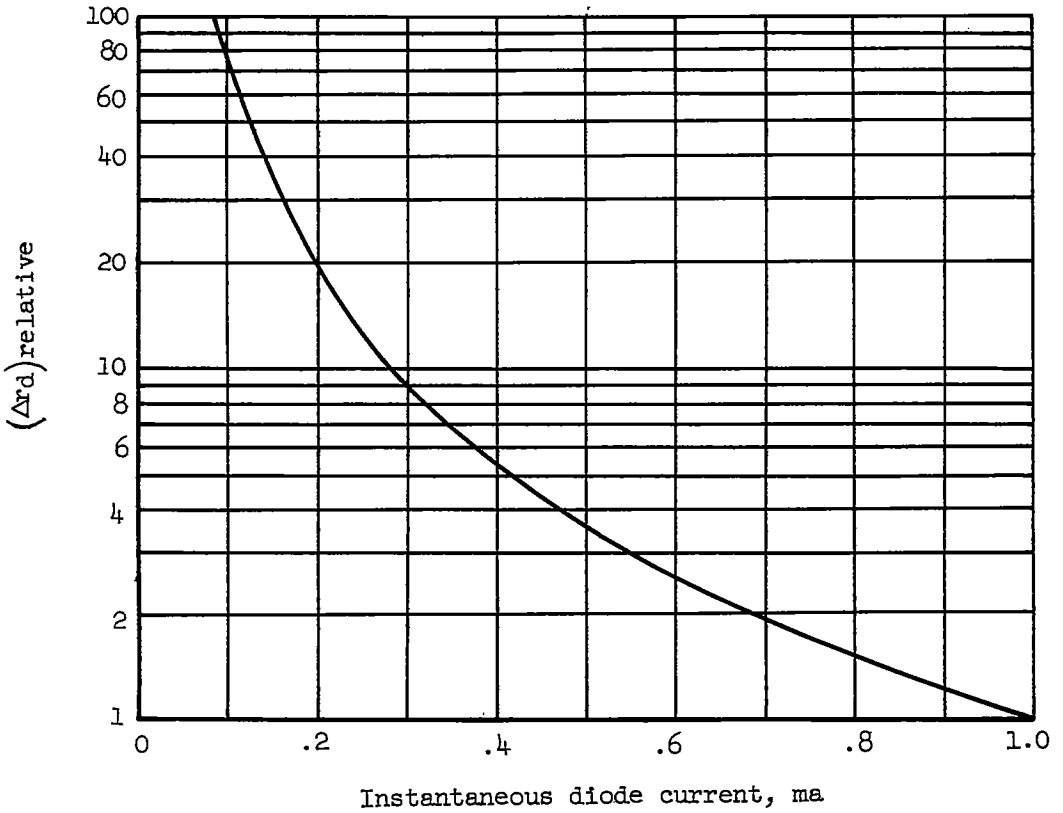

Figure 6.- Relative diode matching.

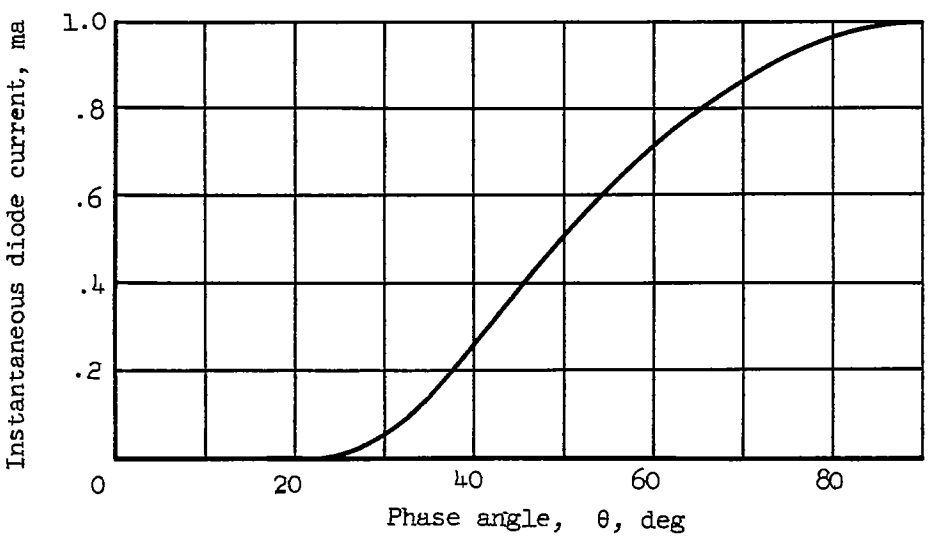

Figure 7.- Diode current as a function of phase angle.

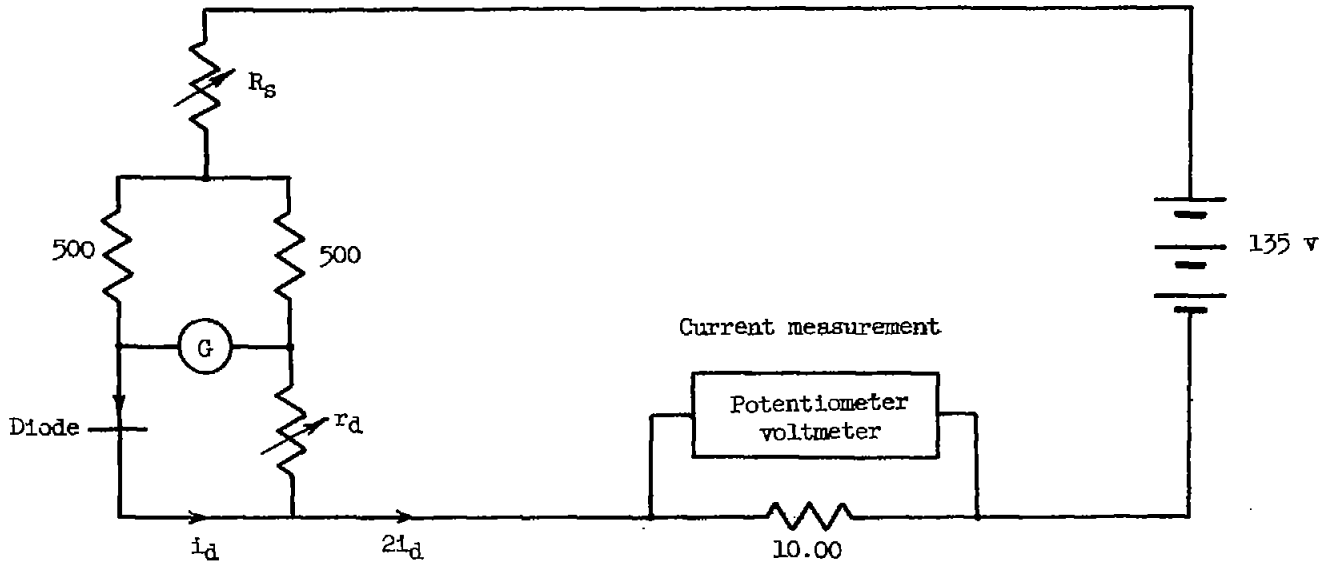

Figure 8.- Circuit for measuring forward resistance at constant values of current. (All resistances are in ohms.)

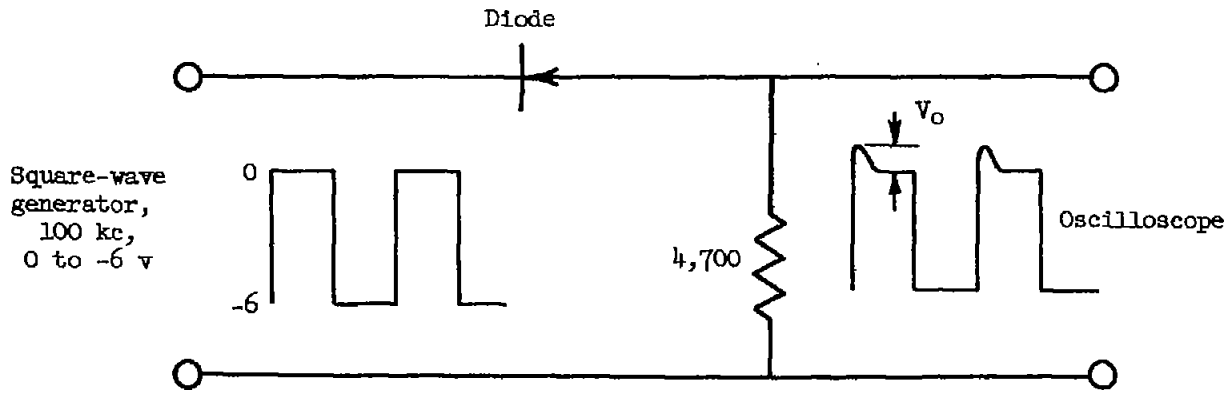

Figure 9.- Capacitance-matching circuit. (Resistance is in ohms.)

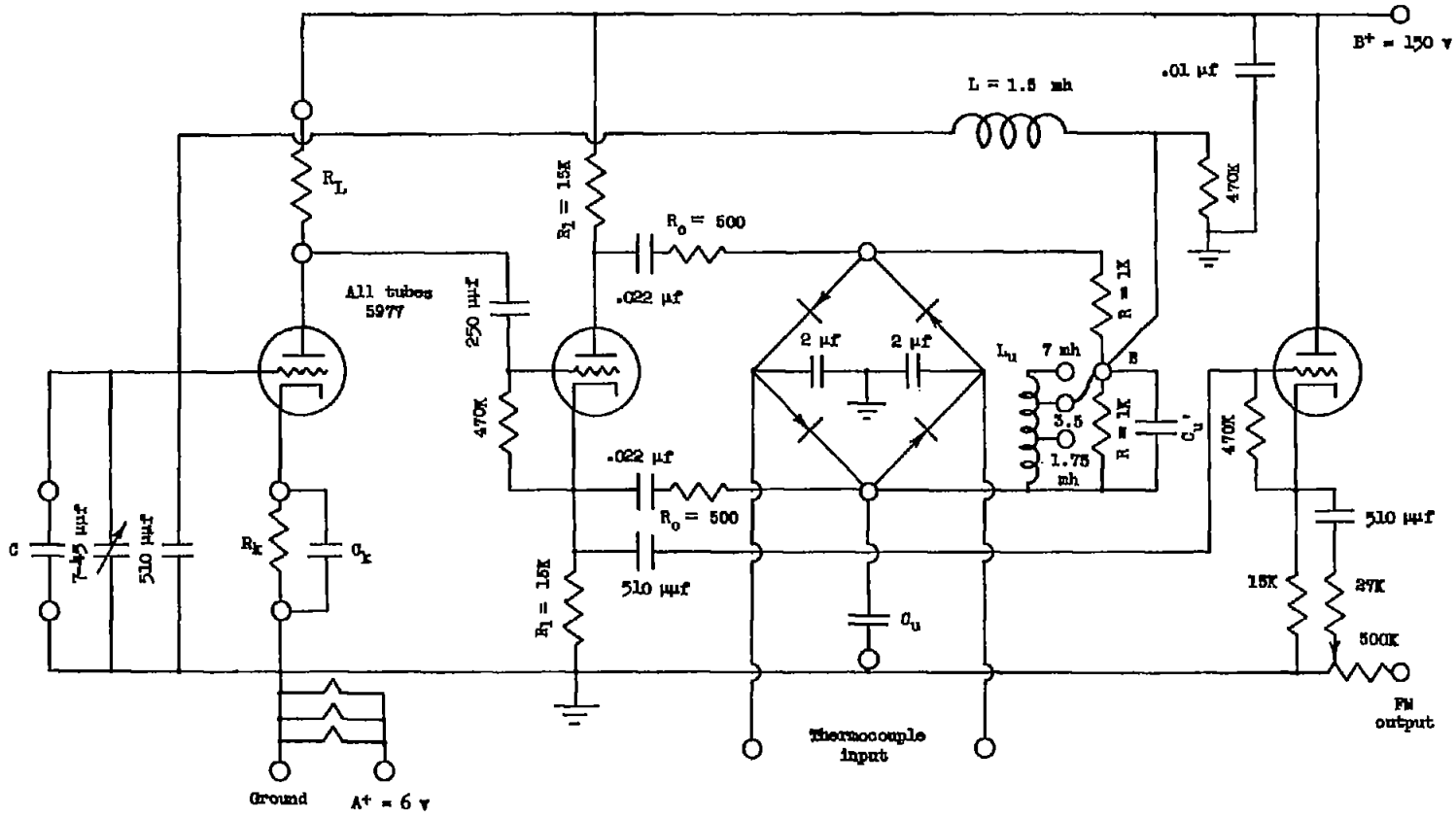

Figure 10.- Schematic diagram of complete oscillator. (All resistances are in ohms; K = 1,000 ohms.)

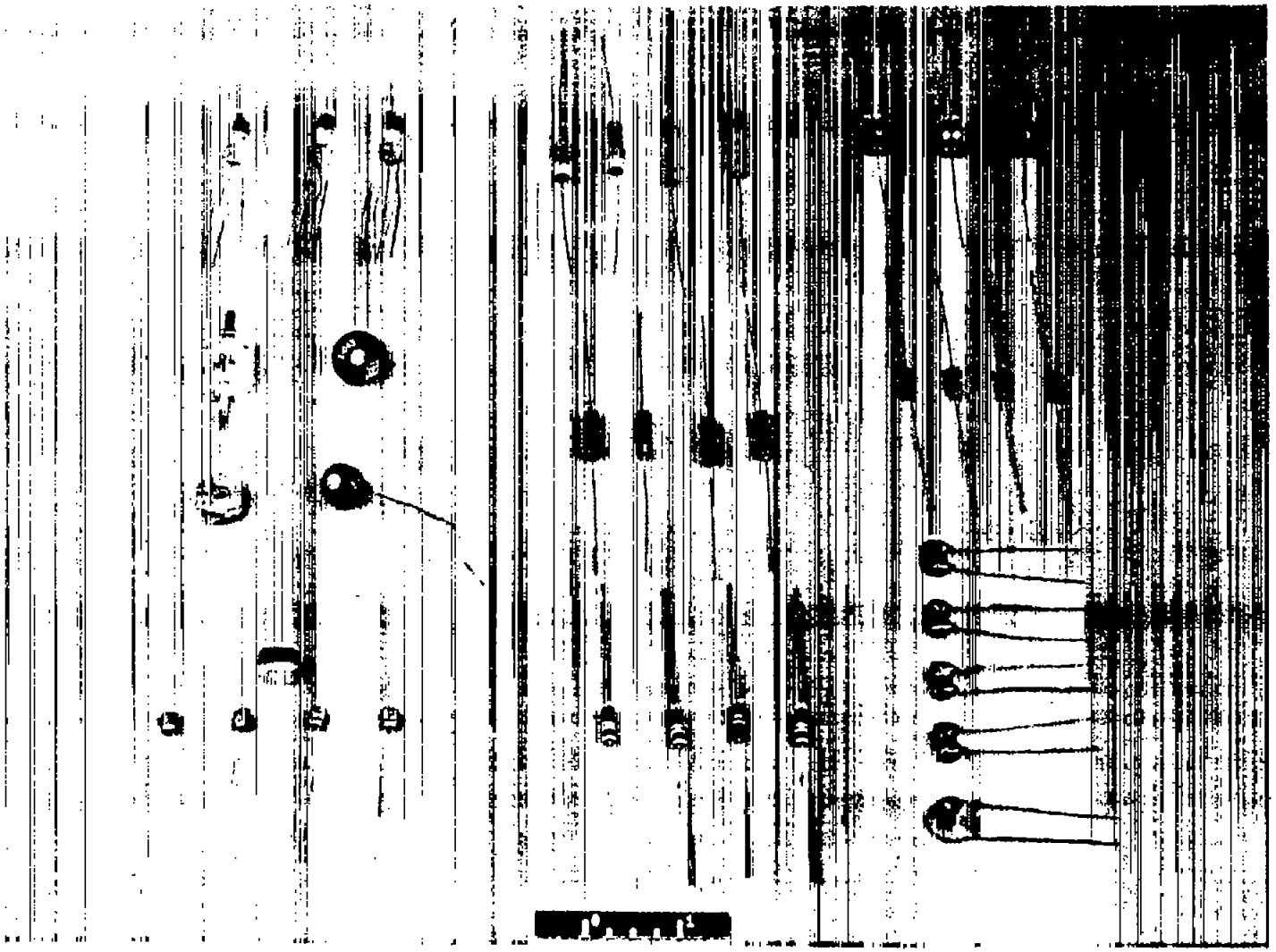

Figure 11.- Electrical components of oscillator. L-57-874

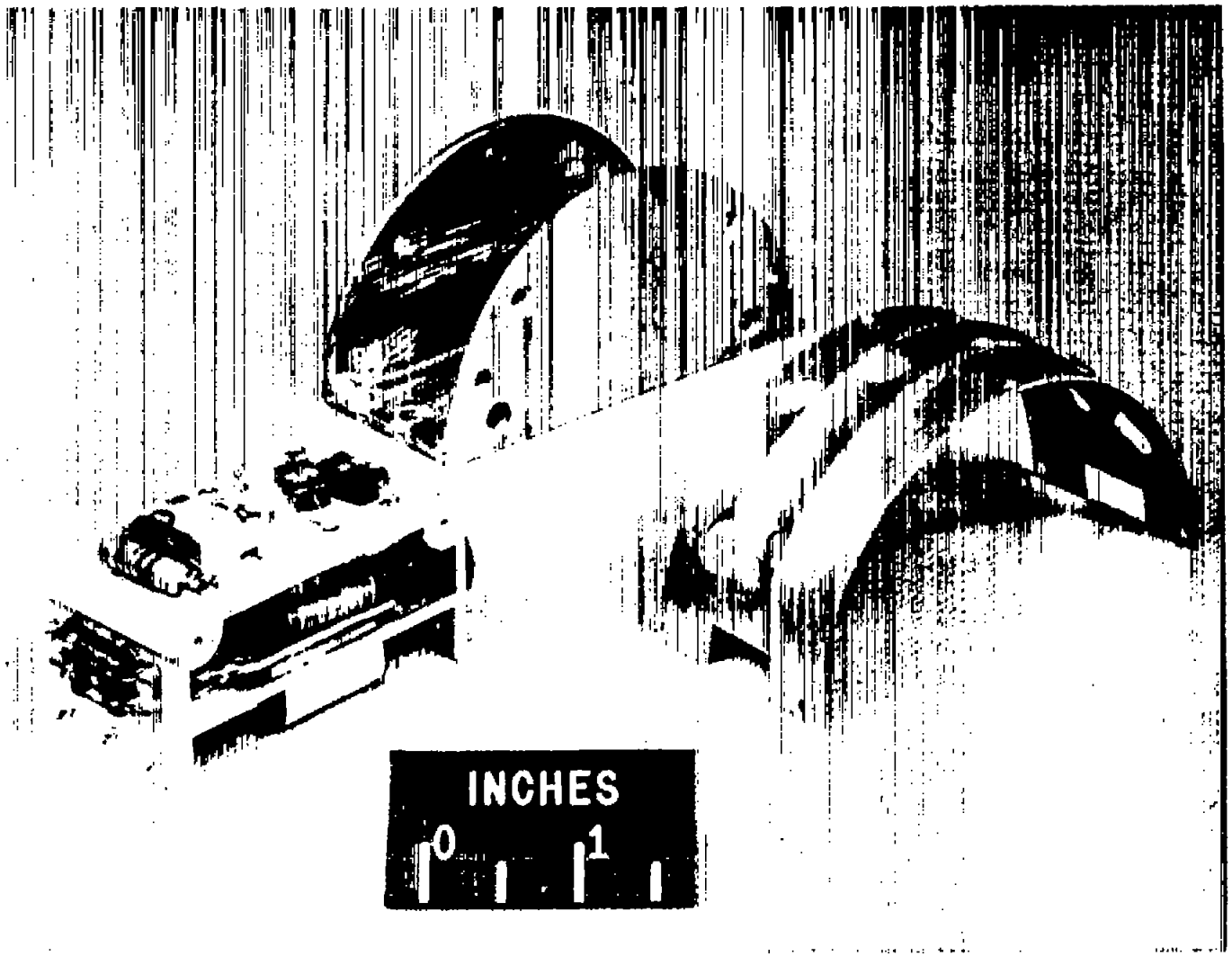

Figure 12.- Complete oscillator with shield can. L-89498

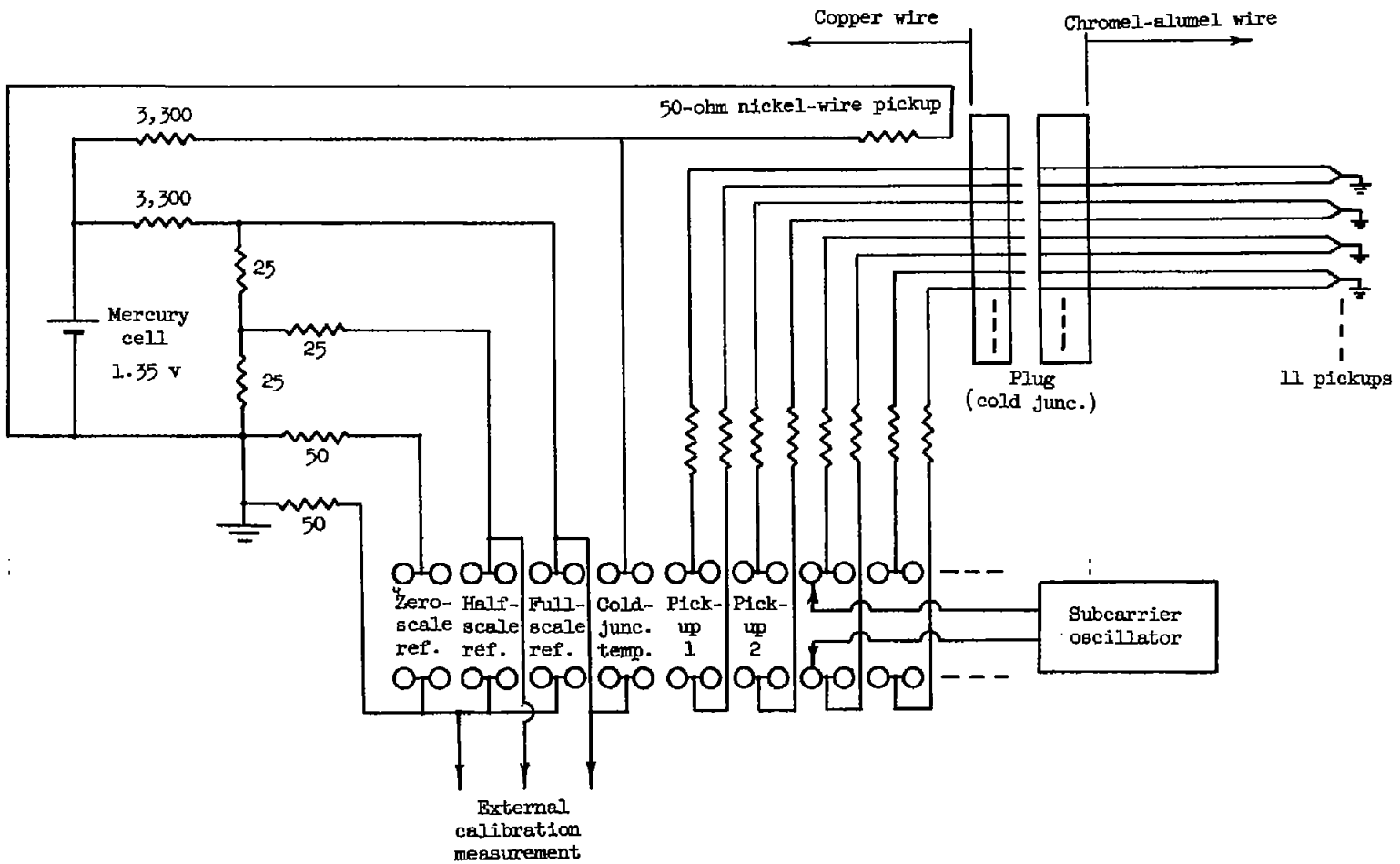

Figure 13.- Diagram of pickup, calibration, and switch circuit. (All resistances are in ohms.)

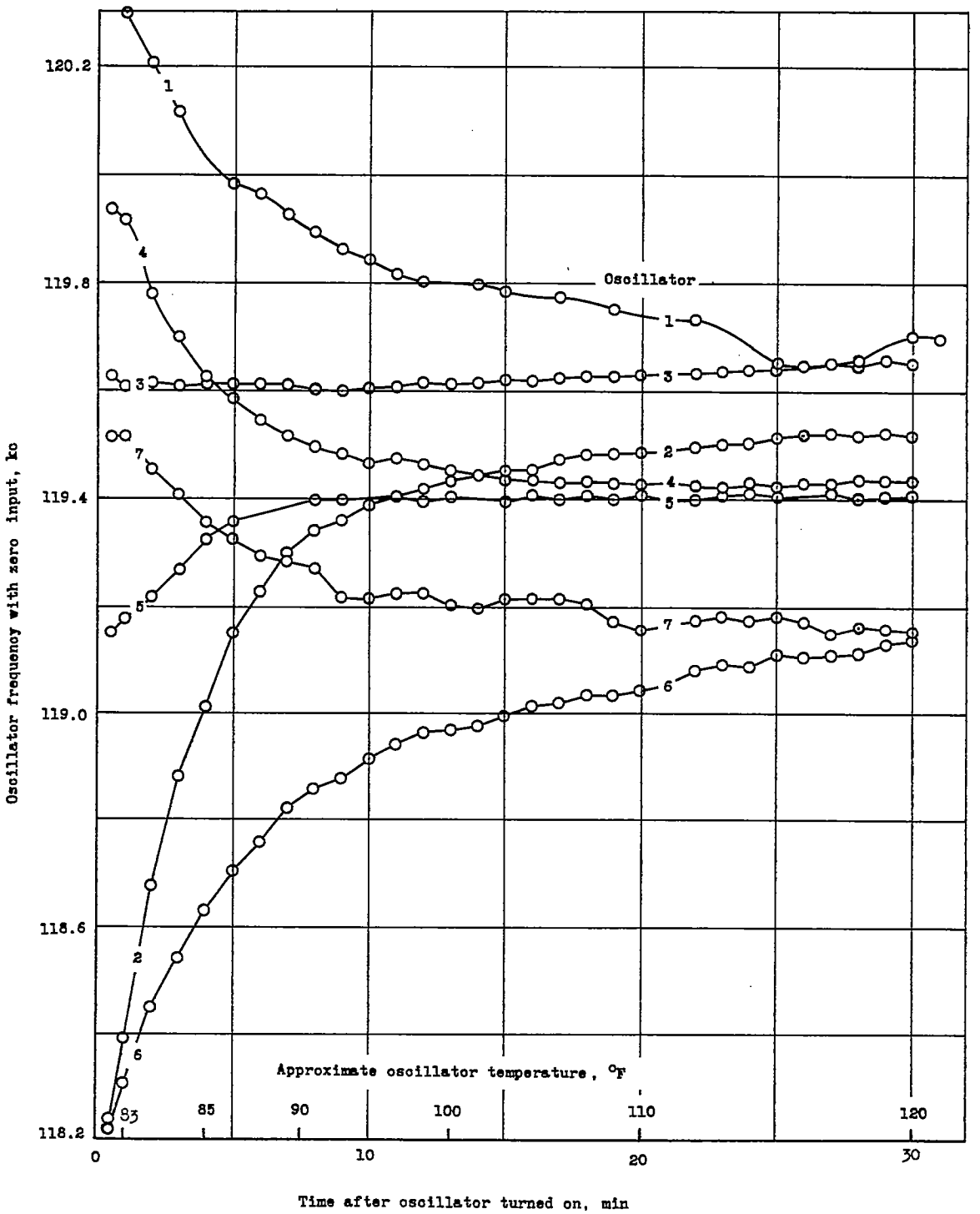

Figure 14.- Warmup drift of oscillators.

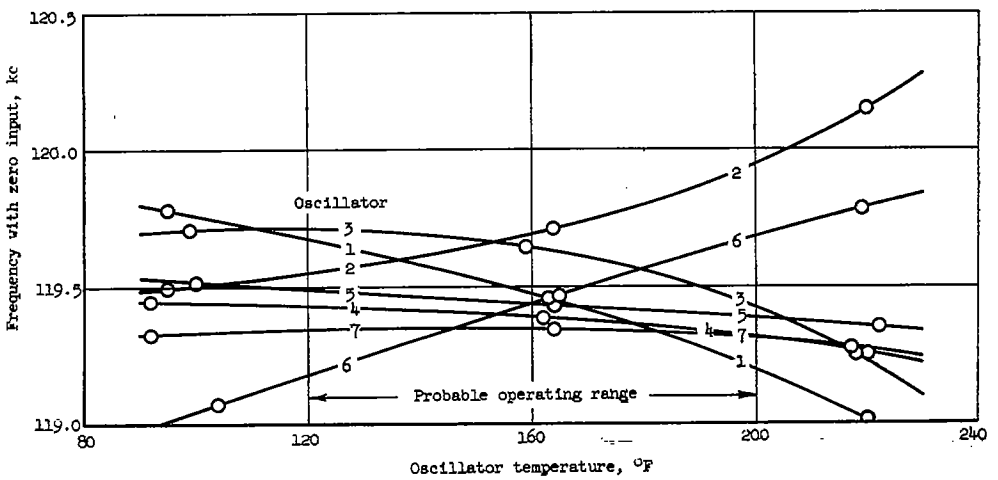

Figure 15.- Zero-input frequency drift with temperature.

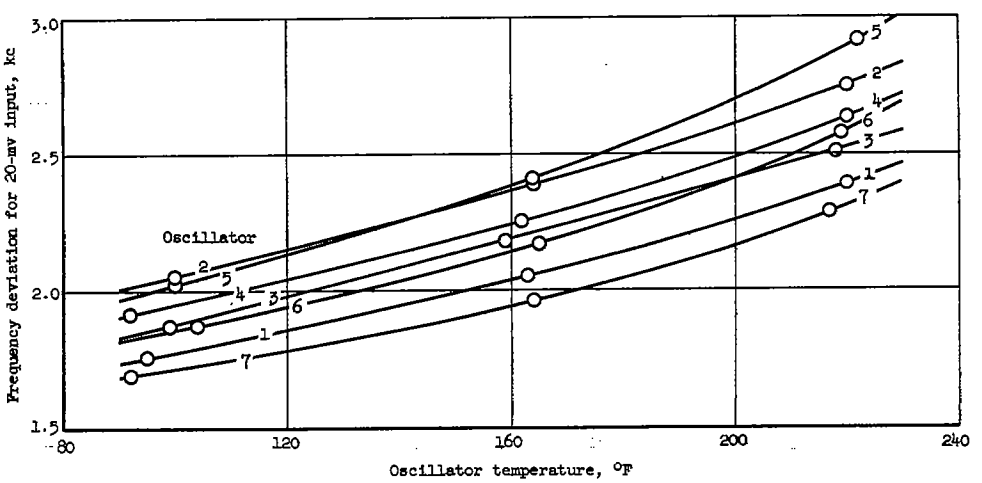

Figure 16.- Sensitivity change with temperature.

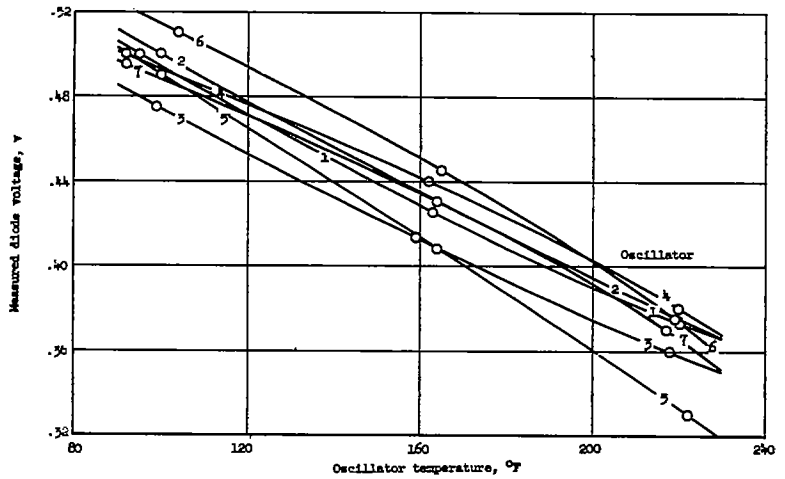

Figure 17.- Diode voltage plotted against temperature.

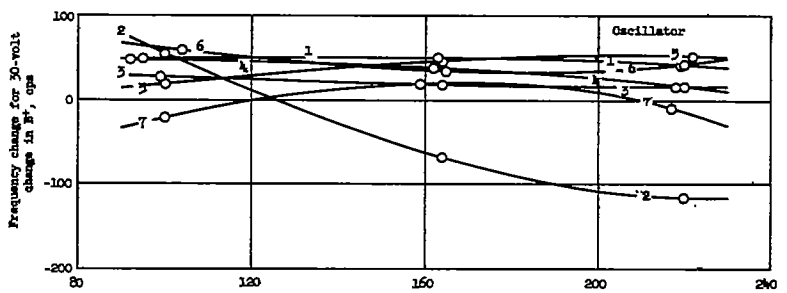

(a) Zero-input shift for 30-volt change in B^+. (B^+ from 150 to 180 volts.)

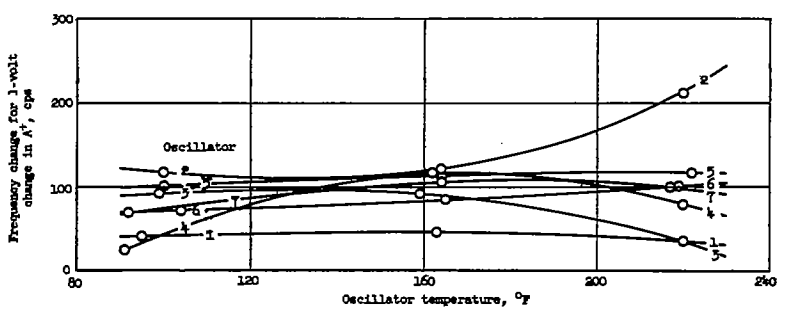

(b) Zero-input shift for 1-volt change in A^+. (A^+ from 6 to 7 volts.)

Figure 18.- Supply-voltage stability with zero input.

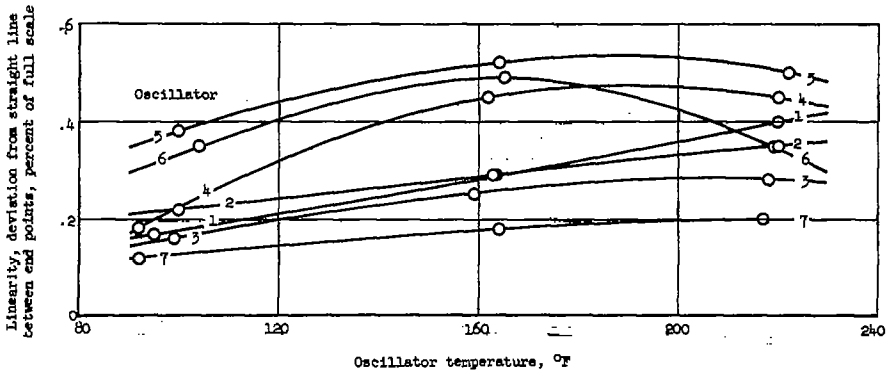

Figure 19.- Linearity of oscillators.

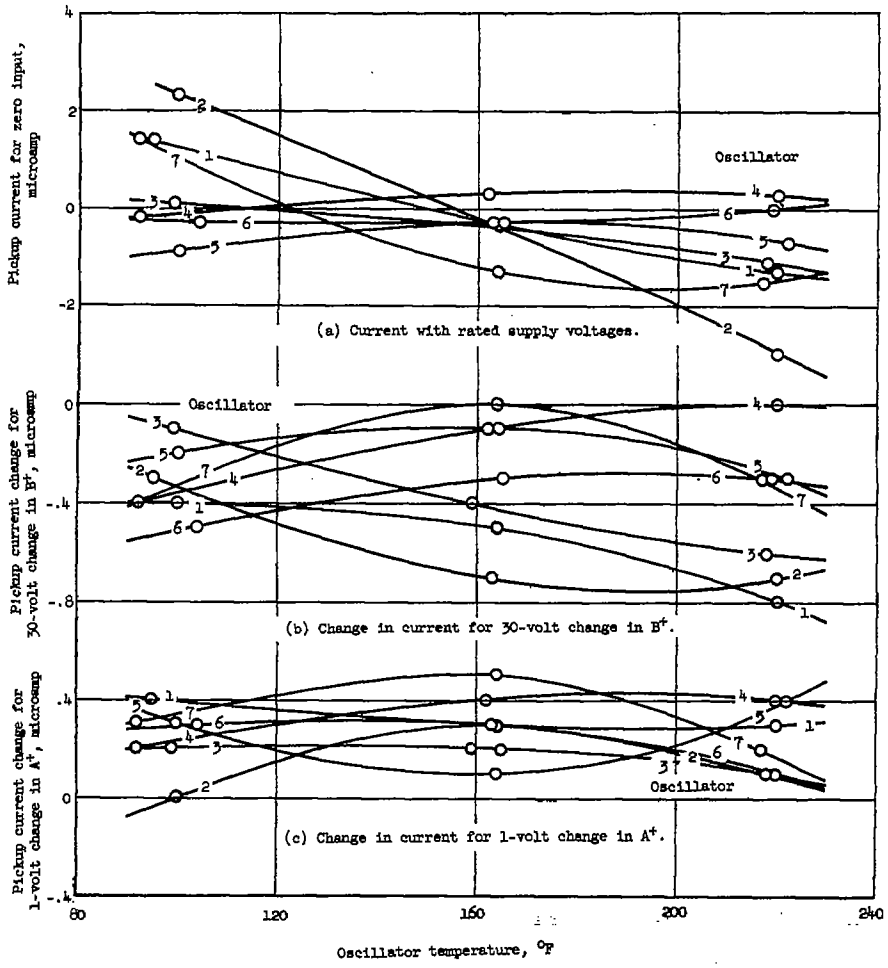

Figure 20.- Pickup current with zero input.

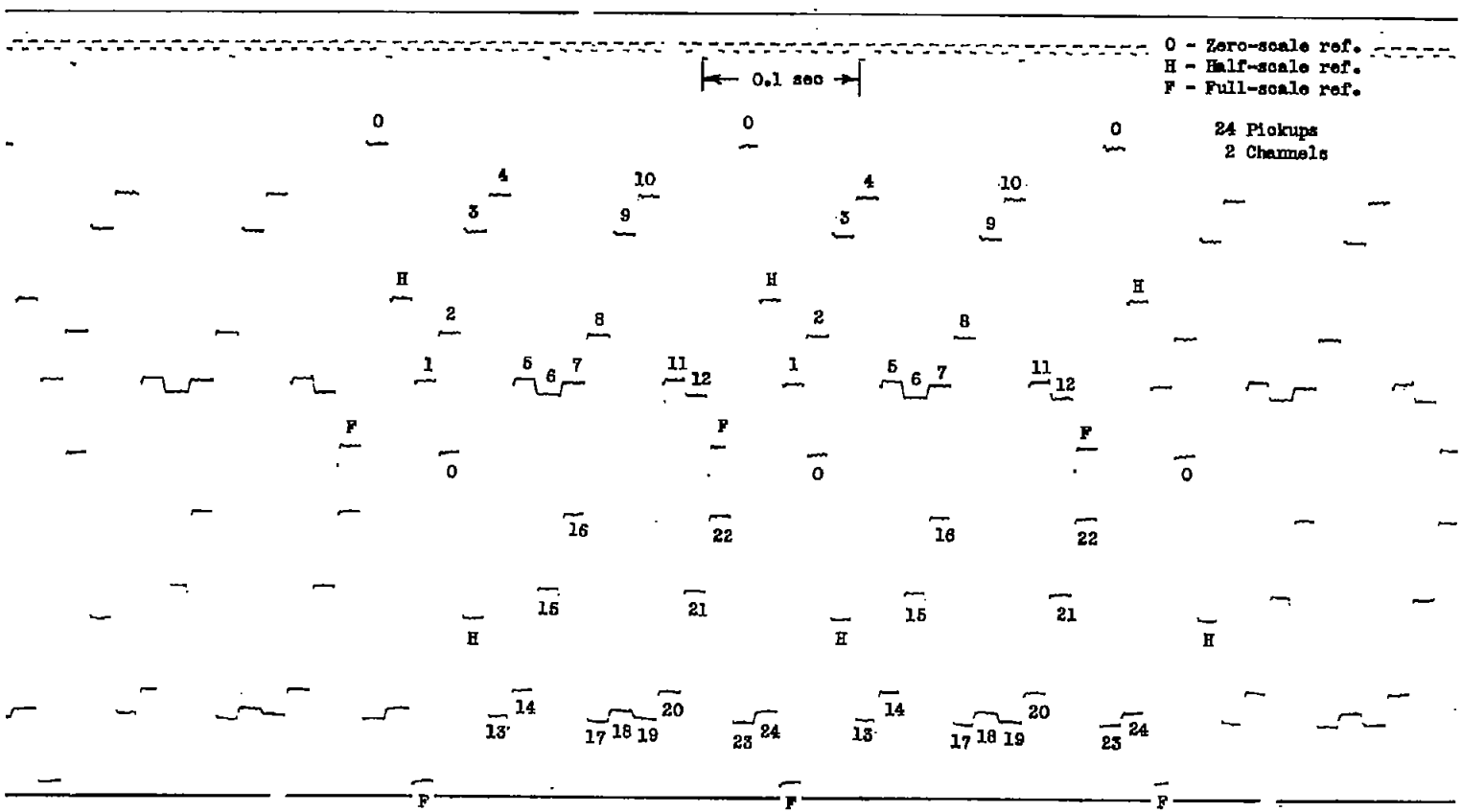

Figure 21.- Actual flight record.

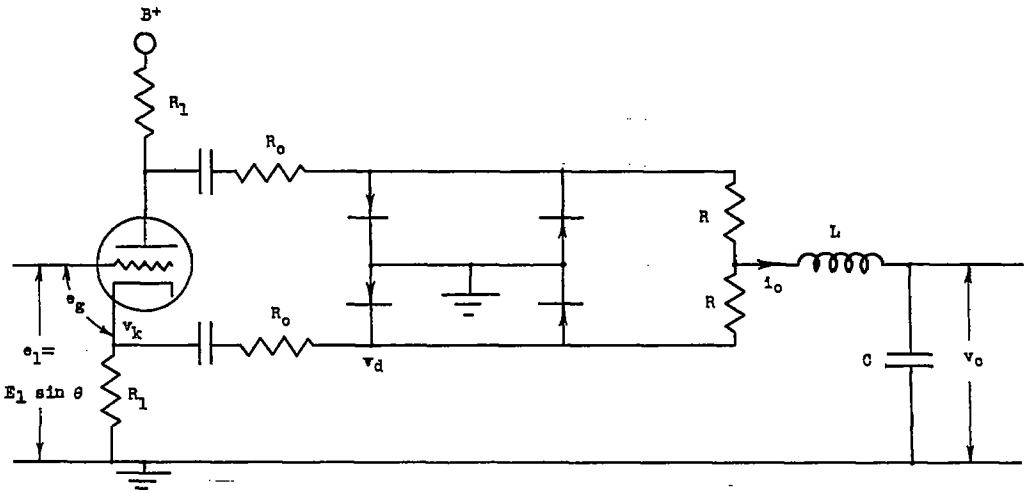

(a) Actual circuit.

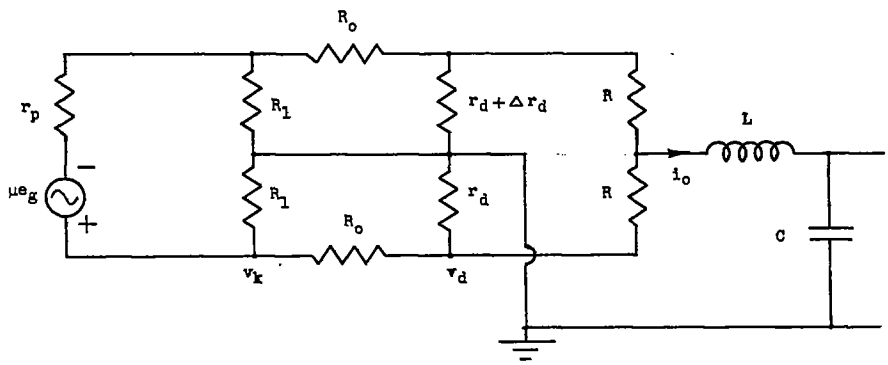

(b) Equivalent circuit.

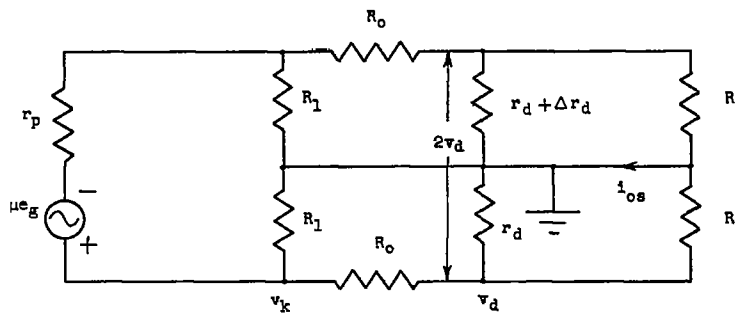

(c) Equivalent circuit with tank shorted.

Figure 22.- Driver, bridge, and tank circuits.